A review of GNSS-independent UAV navigation techniques

Nasser Gyagenda [a],[*], Jasper V. Hatilima [a], Hubert Roth [a], Vadim Zhmud [b]

[a] *Department of Computer Science and Electrical Engineering, University of Siegen, Germany*
[b] *Department of Automation, Novosibirsk State Technical University, Russia*

ARTICLE INFO

ABSTRACT

Application of UAVs (Unmanned Aerial Vehicles) in environments devoid of GNSS (Global Navigation Satellite System) service has motivated research into GNSS-independent navigation solutions. This paper presents an account of such solutions proposed within the last decade. Unlike most literature that abstract UAV navigation to mere localization, this work takes a bottom-up approach by assessing the navigation components namely perception, localization and motion planning presented in the selected literature. The review results indicate that only 16% of the research presented full navigation solutions, while the rest present one or several components thereof. Besides the account of navigation solutions, our other contributions include an adapted MTOW-based (Maximum Take-Off Weight) UAV classification scheme incorporating a nano-sized UAV class, technology maturity assessment of the reviewed GNSS-independent navigation solutions and analysis of integrity monitoring frameworks.

© 2022 Elsevier B.V. All rights reserved.

1. Introduction

UAVs find application in numerous fields that listing them would span quite a footprint. We refer interested readers to articles on UAV applications like [1,2]. The increasing applications have pushed UAVs into complex areas whose control demands exceed human-in-the-loop control capability, which has motivated research into UAV autonomous navigation systems.

Navigation is a speciality of mobile robots. It is a meta-capability, which includes perception, localization, motion planning and motion control. Navigation methods can be categorized with respect to application domain as marine, terrestrial, aerial and space navigation or with respect to technology, which include inertial, vision, radio, acoustic and radar.

The availability of ready to fly off-the-shelf aerial vehicles is testimonial to the mastery of aerial vehicle dynamics and control, but pose estimation especially over long periods still eludes us. The most common pose estimation technique is dead reckoning, but drifts over time, necessitating aiding from other methods, of which GNSS is a common choice, but it is vulnerable to spoofing, jamming, environmental effects [3], absent in indoor, unreliable in urban canyons, natural canyons and forest understories [4,5]. These vulnerabilities have motivated the quest for GNSS-independent navigation solutions.

This paper provides a review of GNSS-independent UAV navigation solutions. It differs from existing reviews by virtual of its scope, assessment of GNSS-independent navigation technology maturity and integrity monitoring. To our knowledge, the existing literature reviews are either narrow in scope, covering a single technique or outdated. For example, the reviews presented in [6–9] report only on vision techniques, [10] relates to navigation only by mention of navigation sensors, [11] provides only a general classification of UAV research and [12] presents a detailed outlook on navigation of unmanned rotor systems up until 2011, which is a decade ago. Our work partially extends [7] in terms of details, but [9] provides a more detailed account of visual localization techniques than is presented here.

The navigation problem is defined as follows: given a starting and a goal point or a set of goal points defined in the same frame of reference, a system should use prior knowledge if available or accumulated knowledge to plan and execute a feasible trajectory from a start to a goal configuration.

2. UAV navigation

Navigation is a meta-capability, which includes perception, localization, motion planning and motion control. Additionally, environmental and mission complexity may necessitate inclusion of obstacle avoidance and mapping. UAV navigation has received a wide spread interest since 2007 with the initial focus on outdoor applications [13], thanks to availability of GNSS services. Soon applications expanded to indoor and other GNSS-denied environments, which necessitated a paradigm shift in the field of navigation.

Starting with UGVs (Unmanned Ground Vehicles) for which GNSS-denied navigation techniques are more mature, attempts to apply UGV navigation solutions directly to aerial navigation

---

* Corresponding author.
  E-mail address: nasser.gyagenda@uni-siegen.de (N. Gyagenda).

Table 1
Navigation research.

Research scope	Papers
Full navigation solution	[4,14–29]
Localization	[5,30–92]
Translational velocity estimation	[93–96]
Approach and/or landing	[48,97–106]
Motion planning	[107]
Obstacle avoidance	[108–110]
Attitude estimation	[111,112]
Mapping	[113]
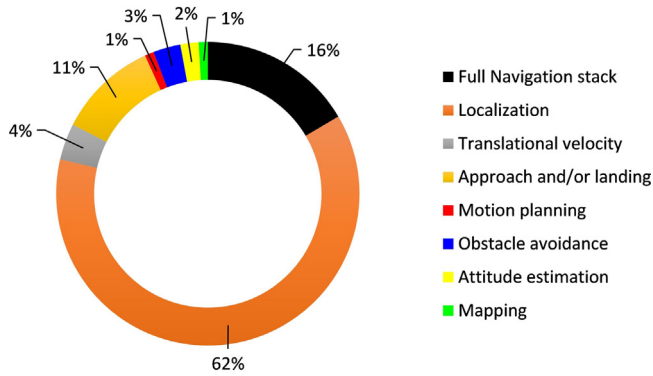
Fig. 1. Distribution of GNSS-independent UAV navigation research.

are limited by the fact that the former operates in a 2D world while the latter operates in a 3D world. Although, the assumption of quasi-fixed operating altitude enables development of 2.5D navigation solutions enabling operation of UAVs in a 3D world with only three controlled degrees of freedom (2D horizontal position and heading) as presented in [5,14], which is comparable to the planar motion of UGVs.

Common to all aspects of aerial navigation is the reliance on state information, which could be available prior to mission e.g. initial state and a map, or acquired during mission execution e.g. distance to approaching obstacles. Localization requires actual state observations and/or initial state information. Motion planning in a closed world requires only a map, whereas motion planning in an open world requires a map for global path generation and real-time state observations for environmental uncertainty minimization. Motion control requires real-time state estimates to stabilize the vehicle. Velocity, heading, altitude, position and attitude are not only the most important states, but also constitute a sufficient input set for navigation.

Autonomous navigation demands the interaction of all navigation components, but due to the sheer complexity of the navigation problem, researchers have focused on addressing individual components as our research reveals in Table 1. As indicated in Fig. 1, localization being a central component of navigation, has received the most attention, followed by approach and/or landing. The downside to this divide-and-conquer approach is that once the individual navigation components are solved, formulating a full solution by aggregation risks exceeding computation, power and hardware capability of any off-the-shelf deployment system. There have also been attempts to solve the full navigation problem, which totalled to 16% of the reviewed literature, showing that there is still a need for full GNSS-independent navigation solutions.

3. Navigation sensors

UAV navigation sensors for GNSS-denied environments can be categorized into attitude, localization, altitude, mapping and

obstacle detection functional categories. Though, some sensors serve more than one category. These sensors can also be characterized as passive or active depending on whether they emit energy into the world. Again, some sensors are both passive and active like RGB-D sensors. Another way to classify these sensors is by technology, where the classes include inertial, vision, LiDAR, radio, radar and acoustic.

Generally, passive sensors are lighter, cheaper and consume less power, but active sensors offer increased measurement accuracy, higher signal-to-noise ratio and robustness against environmental changes. Regardless, it is seldom that a single sensor performs satisfactorily over long periods, hence the need for sensor characterization with the effort to discover complementary sensors. One strategy is to identify sensors that are superior at measuring some degrees of freedom but inferior at others. Other criteria include:

- Error dynamics
- Reliability
- Robustness
- Computational speed
- Exteroceptive or proprioceptive
- Relative or absoluteness
- Representational richness
- Passive or active

3.1. Sensor selection

Selecting the right sensors is a daunting task given its criticality as it lays the foundation for the choice of algorithm, resource usage and performance. Sensor selection criteria include dynamic range, error characteristics, bandwidth, vehicle payload constrains, resolution, response time, operating environment, flight settings, computational resources and power availability.

For non-tactical civilian applications, inertial navigation systems employ small form factor strap-down MEMS-IMU (Micro Electro-Mechanical Systems-Inertial Measurement Unit). A standard IMU consists of a triaxial rate gyroscope and a triaxial accelerometer. The key IMU features are dynamic range, gyroscope in-run bias stability, accelerometer in-run bias stability, gyroscope angular random walk and accelerometer velocity random walk. Inertial sensors have been widely applied to localization, attitude and velocity estimation.

The key vision sensor selection features include resolution, shutter type, maximum frame rate, field-of-view and weight. Spatial deformation and blurring may occur in images as a result of camera motion induced by vehicle motion, vibration and moving objects. Rolling shutter cameras are more affected by this in comparison to global shutter cameras, but could be improved by rolling shutter modelling as demonstrated in [114]. Vision sensors from our review include monocular, stereo, depth, thermal and catadioptric cameras. To ease sharing of experience and code reuse, Table 2 provides a list of cameras applied in the different reviewed articles. Vision sensors have been applied to localization [15,18,28,34,37,43,46,51,55,56,59,62,64,67,68,71–73,78,80], localization and mapping [14,16,17,20,22,24–26,29,41,42,58,63,74,76,81,90,115,116], translational velocity estimation [93,94,96], landing pad detection [97,105], obstacle detection [17,108], attitude estimation [67,111], and landing pad detection and landing [97–99,103–106].

LiDAR rangefinders have either a single fixed or a rotating beam. For the former, important is the range and accuracy. For the latter it is range, accuracy, scan angle, angular resolution and scan speed. LiDAR rangefinders have been applied to height estimation [37,107], obstacle detection and mapping.

The commonly applied acoustic sensor is ultrasonic rangefinder, which is characterized by range, open angle, frequency and accuracy. Ultrasonic sensors operate on time-of-flight

Table 2
Vision sensors applied in the reviewed navigation solutions.

Sensor make	Sensor properties	Papers
Perspective monocular camera		
Pointgrey Chameleon CM3-U3-13S2C	Global shutter, 30 FPS, 54.9 g, 1288 × 964 pixel, CCD	[14,51,54,61]
Pi camera V2	FoV 62.2°, 3280 × 2464 pixel, 3 g, CCD	[15]
UI-1221LE uEYE	Global shutter, 87 FPS, 752 × 480 pixel, 12 g, CMOS	[34]
PointGrey BFLY-PGE-12A2C-CS	Global shutter, 52 FPS, 1280 × 960 pixel, 36 g, CMOS	[16]
Pixy CMUcam5	1280 × 800 pixel, 43 g	[38]
Point Grey Firefly MV	Global Shutter, 752 × 480 pixel at 60 FPS, FoV 150°, CMOS	[76,113]
MV-1300UC-M Industrial Camera	*n/a*	[41]
Canon IXUS 125 HS	1920 × 1080 pixel at 30 FPS, 320 × 240 pixel at 240 FPS, CMOS, 135 g	[46]
UI-1641LE - uEye	640 × 480 pixel, CMOS	[94]
QuickCam Pro 4000 USB camera	Global shutter, 1280 × 960 pixel, 25 g, CCD	[97]
AVT Prosilica GT-1380	Global shutter, 30.5 FPS, 1360 × 1024 pixel, 211 g	[54,116]
PointGrey Flea2	15 FPS, 69° × 54° FoV, 1384 × 1032 pixel	[54]
mvBlueFOX-MLC	Global shutter, 752 × 480 pixel, 93 FPS	[64,78]
KX-171	25 FPS, 320 × 240 pixel	[72]
GoPro7	3840 × 2160 pixel at 60 FPS	[79]
PlayStation Eye	640 × 480 pixel at 20 FPS, 150 g	[79]
Genius WideCam F100	1920 × 1080 pixel at 30 FPS, 82 g	[106]
FLEA3 FL3-U-20E4C-C	Global shutter, 1600 × 1200 pixel at 59 FPS	[110]
Stereo camera		
ZED	Depth 0.3 − 25 m, 3840 × 1080 pixel at 30 FPS, rolling shutter, 135 g	[115]
In-house	AVT MARLIN F-131B cameras, 30 FPS, 1280 × 960 pixel, global shutter, baseline 0.3 m	[56]
Minoru 3D webcam	800 × 600 pixel at 30 FPS, baseline 0.06 m, FoV 42°	[87]
Parrot S.L.A.M.dunk	30 FPS	[83]
Omnidirectional camera		
In-house catadioptric sensor	FD-1665P polarization camera	[111]
In-house multi-camera system	FoV 360°	[67]
Depth camera		
Asus Xtion Pro Live	Depth Image Size: VGA (640 × 480) pixel at 30 FPS, QVGA (320 × 240) pixel at 60 FPS, RGB 1280 × 1024 pixel, depth 0.8 m − 3.5 m	[20,43]
Intel Realsense R200 camera	640 × 480 pixel, 60 FPS, depth 0.5 m–3.5 m	[19]
Intel Realsense ZR300	480 × 360 pixel, depth 0.55 m–2.8 m, IMU	[70]
Microsoft Kinect	Depth 0.4 m–4.5 m, 640 × 480 pixel at 30 FPS, FoV 57° × 43°	[22,81]
Occipital Structure core	0.3 m–5 m (Up to 10 m depending on scene and lighting) depth, 0.3 MP, global shutter, 52.5 g	[87]
Orbbec Astra	1280 × 800 pixel at 30 FPS, depth 0.25 m–1.5 m	[25]
Thermal camera		
Optris PI 450	382 × 288 pixel, 80 FPS	[16]

principle with range given as $0.5 \times C \times t$, where C is the speed of sound. Since C is affected by temperature, pressure and humidity, with temperature having the greatest influence of all [117], it is necessary to account for them to obtain accurate ranging.

Generally, inertial sensors are proprioceptive, have high update rates of up to 1 kHz [118], score highly on SWaP-C (size, weight and power - cost) scale, but drift. Vision sensors are less effective for long-range perception, low illumination and low textured environments [50], exhibit lower update rates, normally under 100 Hz [118], but capture diverse information, are lighter and relatively cheaper. LiDAR rangefinders are relatively expensive, heavier and exhibit degraded performance under bad weather conditions and direct sunlight [119], but deliver more accurate, direct and longer-range high frequency measurements. Radar sensors are relatively bulky and consume the most power, but deliver the longest-range and are insensitive to environmental conditions.

3.2. Motion capture systems

When sensing is not the focus, motion capture systems can deliver direct state tracking information. They consist of synchronized active–passive optical sensors strategically positioned to accurately track objects within a pre-defined volume. The three ways motion capture systems were used in the reviewed literature include localization, absolute position initialization and ground truth for state estimator performance evaluation. The

downsides to these systems are high cost and limited measurement volume [42]. The different motion capture systems from literature are depicted in Table 3, all of which are marker-based.

4. Localization

Localization answers the "where am I?" question by estimating the vehicle position. This capability is not only necessary for navigation, but also for object manipulation, multi-robot coordination, exploration and mapping. As revealed in Fig. 1, it is the most researched navigation component.

Robots are situated agents [121,122]. This situatedness supports perception affordance for inertial, visual, radar, radio, LiDAR and acoustic-based localization. As presented in Table 4, each localization technique exhibits benefits and drawbacks. Drawing from complementarity, localization solutions combining multiple techniques have yielded better performance. As will be seen throughout this paper, such hybridizations are a powerful and common strategy.

Localization techniques require environmental representations, which could be made available beforehand in form of geo-referenced aerial images [46,77], CAD (Computer-Aided Design) models [83,87,91], DTMs (Digital Terrain Models) [67], occupancy grid maps and feature maps [37,45], or built and used simultaneously, as in SLAM (Simultaneous Localization and Mapping) [122]. Environmental representations could be generated simply by embedding artificial beacons at known positions in the environment [62,86], which are then tracked by on-board sensors. The

Table 3
Motion capture systems.

Motion capture system	Usage	Papers
Vicon	Performance evaluation	[14,70]
OptiTrack	Performance evaluation	[19,34]
	Localization and attitude estimation	[71,96]
Qualisys	Performance evaluation	[120]
Motion analysis	Performance evaluation	[20]
	Position initialization	[20]
In-house system (five Kinect sensors network)	Localization	[81]

Table 4
Pros and cons of the different localization technologies.

| Mode	Pros	Cons
Inertial	• Very low SWaP (Size, weight and power) • Low cost • Very high update rate • Very short start-up time • Jam proof	• Drifts over time • Low signal-to-noise ratio at low acceleration and angular velocity • Quality dependent on knowledge of initial state
Vision	• Light weight • Semantic information • Jam proof	• Affected by weather and illumination • Indirect state observation • High computational load
Radar	• Longest operating range • Robust against illumination and weather • Direct measurements • Range independent resolution	• Costly • Bulky • High power consumption • May require environmental accessories like transponders or reflectors
Ultra wideband (UWB)	• Weather independent • Provides a communication channel • Low power consumption	• Interference from conductive materials • May require environmental installations • Limited operating volume/range • Low update rate circa 10 Hz
Magnetic	• No environmental installation • Very low power consumption • Low cost	• Susceptible to magnetic interference • Requires delicate calibration • Low precision
LiDAR	• No environmental installation required • Very precise • Direct measurements • High update rate	• Very costly • Degraded by direct sunlight • Influenced by reflecting surface properties, like colour • Limited range, less 100 m

opposite is also possible, where beacons are mounted on the vehicle and sensors fixed in the environment [71,81] as is the case with marker-based motion capture systems. This concept has been extended to multi-robot localization. An example is [32] where a vehicle in a GPS-denied environment localizes itself relative to GPS-enabled vehicles.

Aerial images are the most popular environmental representations, but finding image representations that are illumination invariant and tolerant to slight view point changes is challenging. Proposed solutions to address the former include image gradient patterns [51] and learned features [46], and appearance-based matching methods [123] for the latter. For a summary of localization techniques see Table 5 and for the distribution of localization techniques among full navigation solutions see Fig. 2.

4.1. Inertial localization

UAV inertial localization operates on the principle of dead reckoning, where accelerations and/or velocities are integrated over time to obtain vehicle position and orientation with respect to an inertial reference frame. As mentioned in Section 3, inertial systems employ IMUs, which exhibit high update rates making them suitable for agile vehicles like UAVs. However, integration causes drift.

To address drift, it is customary to fuse inertial with other complementary techniques like vision, for example VIO (Visual
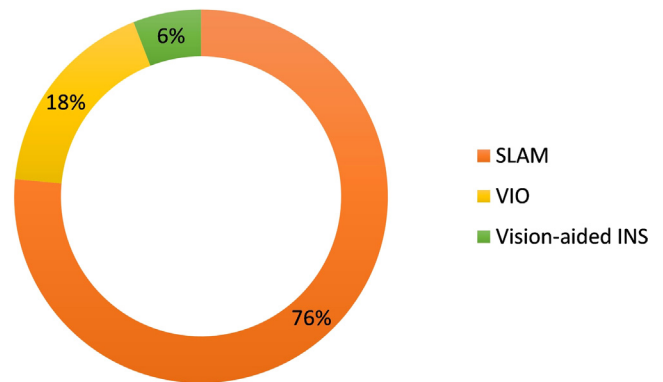
Fig. 2. Distribution of localization techniques among reviewed full navigation solutions.

Inertial Odometry) as described in [118], visual odometry and optical flow, PARS (Phased Array Radio System) [30], LiDAR [5] and UWB [57] through state estimators like Kalman or particle filters. Fusion could happen at raw data or state level, known as tightly coupled and loosely coupled schemes respectively. Disparate performance studies have concluded that tightly coupled schemes are more accurate and robust than loosely coupled schemes [118,124], but more complex and inflexible [66].

Table 5
Practically tested localization solutions.

Localization	Aiding technology	Papers
LiDAR SLAM	n/a	[14,19,21,23,27,50,69,88]
Visual SLAM	n/a	[4,16,17,20,24–26,41,42,54,76,83,87,90]
Visual inertial odometry	n/a	[18,22,28,29,58,59,68,72,74,79,84,116]
	GPS	[56]
Air-to-air cooperation	GPS and vision-based bearing	[32]
INS	VO	[31,47]
	PARS	[30]
	Artificial markers	[15,43,55,70,78,86]
	Machine learned vehicle model	[39]
	LiDAR scan matching	[5]
	UWB and vision	[56]
	Artificial immune system (AIS)	[82]
Beacons	Visual beacons	[34,80]
	Radar beacons	[35]
	UWB	[36]
Knowledge-based localization	Radar propagation channel response	[45]
	Satellite image	[46]
	CAD model	[91]
Radar odometry	n/a	[66]
Motion capture system	n/a	[71,81]

Table 6
Full navigation solutions.

Paper	Perception	Environment	Localization	Path planning	Obstacle avoidance
[14]	Vision, laser rangefinders, IMU	Known indoor	2D SLAM	A*	Online local path planning
[15]	Vision, IMU	Known outdoor	Visual-aided INS	Ground control points	n/a (not available)
[16]	Vision, laser rangefinders, IMU	Unknown cluttered outdoor and indoor	2D SLAM	A*	Online local path planning
[4]	Vision, IMU	Unknown, unstructured	Visual SLAM	POMDP motion planner	Raycasting
[17]	Vision, IMU, sonar	Indoor and outdoor	Visual SLAM	A*	Obstacle grid map
[18]	Vision, IMU	Structure known indoor	VIO	POMDP motion planner	Online local trajectory generation
[19]	Vision, laser rangefinders, IMU	Indoor	2D SLAM	n/a	Online local path planning
[20]	Vision, sonar, IMU	Structure indoor	Visual SLAM	Dijkstra's algorithm	Online path re-planning
[21]	Vision, laser rangefinders, IMU	Indoor	2D SLAM	A*	Artificial potential fields
[22]	Vision, sonar, IMU	Unstructured, partially known indoor	Visual SLAM	BI-RRT	Obstacle free global path
[23]	Laser rangefinders, IMU	Unstructured, unknown indoor and outdoor	LiDAR SLAM	n/a	Laser-based obstacle mapping
[24]	Vision and IMU	Complex indoor and outdoor	Visual SLAM	Dijkstra's algorithm	Obstacle free global path
[25]	Vision and IMU	Known indoor	Visual SLAM	Weighed Lazy Theta*	Online local path planning
[26]	Vision and IMU	Partly known indoor	Visual SLAM	A*	Online local path planning
[27]	Vision, laser rangefinders, IMU	Partly known indoor	LiDAR SLAM	A*	Obstacle free global path
[28]	Vision and IMU	Cluttered indoor and outdoor	VIO	Dijkstra's algorithm	Online local trajectory generation
[29]	Vision and IMU	Cluttered unknown indoor and outdoor	VIO	A*	Online local trajectory generation

Results from this study accentuate the indispensability of inertial techniques in any modern GNSS-independent navigation solution with 100% presence in full navigation solutions as indicate in Table 6, aided by other techniques to minimize drift. It is also evident that vision is the most popular inertial aiding method with over 94% presence. It is our conviction that inertial–visual integration holds the key to GNSS-independent navigation solutions of the future.

4.2. Visual localization

Visual localization utilizes vision sensors and computer vision to extract location information from visual scenes. Its popularity is attributed to the low weight and power consumption of vision sensors, as well as their rich environmental representation, which includes shapes, colour and texture. However, vision algorithms are affected by illumination variations, low feature density, motion blurring and consume relatively high computational resources.

Vision methods are categorized as indirect aka feature-based or direct aka appearance-based methods [125,126]. The former abstracts images to features making it faster while the latter operates directly on image pixel intensities, a trait that results in improved robustness against illumination variations. Of the two,

feature-based methods are more popular given their lower computational cost, sparsity and robustness against rolling shutter artefacts [126], but exhibit degraded performance in featureless environments. It is also possible to combine indirect and direct methods resulting into semi-direct methods [9,127].

Essential to indirect methods is the choice of features. Features either occur naturally in the environment or are specially designed and embedded into the environment to ease computer vision processing. Table 7 presents a summary of features identified in the reviewed literature and their associated properties.

To localize, correspondence must be established between features in consecutive frames, either by (1) detecting features in one frame and tracking them into a local region in the next frame or (2) detecting features in multiple images and matching them based on local similarity [128]. The former finds application in sparse optical flow, feature-based visual-SLAM and feature-based visual odometry while the latter finds application in image matching as in establishing correspondence between a large-scale image (e.g. satellite images) and a small-scale image for terrain-based localization [46]. Table 8 presents two sets of computational speed tests for FAST, SIFT, SURF, ORB, shi-Tomasi, Harris corner detectors, both of which indicate FAST feature detector as the fastest.

As indicated in Fig. 2, visual localization, specifically SLAM dominates among full navigation solutions. This dominance is

Table 7
Visual features.

Features	Properties	Papers
FAST/ORB	• Computationally fast • Accurate • Rotation, scale and global illumination invariant • High repeatability	[20,31,60]
SIFT	• Scale and rotation invariant • Computationally slow	[41,63,73]
SURF	• Scale and rotation invariant • Computationally slow (faster than SIFT)	[46,58,61,68]
Shi-Tomasi	• Scale and rotation invariant • Based in Harris corners with better selection criteria	[55]
AGAST	• Derived from FAST features • Computationally fast • Dynamically adapting corner detector	[24,28]
Harris corners	• Rotation invariant • Intensity shift invariant • Intensity scaling invariant • Sensitive to image scaling	[74,110,116]
Solid circles	• Easily identifiable • Embed scale information	[34,38]
Lines (edges or horizon)	• Easy to extract from noisy images • Orientation of lines may be estimated with sub-pixel accuracy • simple mathematical representation	[5,67]
Semantic features • Doors • Roads (intersection and centreline)	• Semantic understanding • Complicated mathematical definitions • Strong localization information	[55,59,65]
Learned features	• Not limited to human interpretation • Generalize well • Robust across heterogeneous images	[19]

Table 8
Feature detector speed tests.

Papers	Time (ms)					
	FAST	ORB	SIFT	SURF	Harris Corners	Shi-Tomasi
[22]	**2.8**	15.6	91.1	112.3	16.7	*n/a*
[95]	**4.1**	*n/a*	33.4	23.6	*n/a*	16

attributed to its ability to simultaneously map and localize a vehicle in an unknown environment. SLAM rely on loop closure to reduce drift [58,63,76], however, loop closing cuts on the overall flight time. It should also be mentioned that SLAM initialization is a delicate step, which if not executed well can affect localization quality. SLAM initialization methods found in literature include use of GPS [60], GPS/INS [54], pre-stored map [113], feature points [50] and manual flight initial mapping [98]. Detailed accounts of UAV visual localization can be found in [8,9].

4.3. LiDAR localization

This employs laser rangefinders, which actively illuminate the environment with a collimated light beam capable of measuring depth to a single point, a feature lacking in wide open angle sensors like ultrasonics. Single beam laser rangefinders have been applied to AGL (Above Ground Level) ranging in [37,107]. With a rotating and/or nodding mechanism, they can also generate 2D and 3D localization point clouds respectively.

Unlike vision sensors, laser rangefinders provide direct ranging, but miss scene texture and colour, making them complementary to cameras that capture such information. This complementarity has been exploited in [14,16,19,50,69] for UAV localization. Table 9 lists LiDAR sensors from the reviewed literature.

4.4. Radio localization

This section describes localization solutions supported by radio technology, which from the reviewed literature include radar, UWB (Ultra Wide-band) and PARS (Phased Array Radio System).

4.4.1. Radar localization

Until recently, radar SWaP constraints had limited its usage to normal and large aerial vehicles, but with recent technological breakthroughs, miniaturized radar modules fit for small UAVs are starting to emerge, and hence the associated radar localization solutions.

A demonstration of radar transponders deployed by a UAV at the onset of landing phase is presented in [35]. The transponders together with a multi-channel radar sensor constitute a wireless local positioning system. The position of on-board radar sensor is determined from range and elevation measurements to each of the transponders. Although the applied transponders are small in size (0.035 m × 0.015 m), the on-board dome sensor is quite bulky and heavy at 0.280 m × 0.290 m × 0.285 m and 1.78 kg respectively.

Biological inspiration is a driving factor in a number of robotic solutions, from anthropomorphic appearance of humanoid robots to evolutionary algorithms. Inspired by echo location in cave swiftlets, [45] used an FMCW (Frequency Modulated Continuous Wave) X-band radar transceiver mounted on a UAV to map propagation channel responses of the environment pre-flight. During localization, the vehicle position is determined from the closest match between the actual and stored channel responses. This localization technique was found have high sensitivity to antenna orientation differences during reference channel response gathering and localization, making it lacking in robustness.

The proof-of-concept in [66] investigated radar-only 2D-localization of UAVs using radar odometry. An ultralight FMCW

Table 9
LiDAR sensors.

Dimensions	Brand	Papers
1D	LiDAR Lite v1 and v3 (0 m–40 m, 0.022 kg)	[70,79,88]
	Lightware SF10/A (laser rangefinders, 25 m, 32 Hz, 0.035 kg)	[19]
	TeraRanger One (14 m, 6 m in sunlight, 0.008 kg, 3°, 10–12 V)	[14]
	TeraRanger Evo mini (0.03 m − 3.3 m, 0.009 g, 27° FoV)	[129]
2D	Hokuyo UTM-30LX (0.1 m–30 m, 270°, 40 Hz, 0.25° angular resolution, 0.37 kg)	[5,16,19,21,23,54,63,88, 130]
	Hokuyo UST-20LX (0.06 m–20 m, 270°, 40 Hz, 0.25° angular resolution, 0.13 kg)	[14,27]
	RPLIDAR A2 (0.15 m–12 m, 360°, 1° angular resolution, 10 Hz, 0.19 kg)	[79,109]
	Hokuyo URG-04LX (0.06 m–4.0 m, 240°, 0.36° angular resolution, 10 Hz, 0.16 kg)	[69,88]
3D	Velodyne LiDAR Puck Lite (3D, 100 m, FoV 360° H, ±15° V, 5 Hz − 20 Hz, 0.59 kg)	[131]

radar transceiver with one transmitter antenna and two receiver antennas mounted on a UAV measures azimuth and range to multiple static corner reflectors in the environment. OS-CFAR (Ordered Statistics-Constant False Alarm Rate) detector was applied for target detection and GNN (Global Nearest Neighbour) algorithm for multiple corner reflector tracking. This technique had difficulty differentiating rotation-only from translation-only motion. Furthermore, despite designation as ultralight, the applied SENTIRE Radar transceiver is relatively heavy, weighing 0.186 kg.

Unlike [35] with deployable transponders and on-board multi-channel radar sensor, and [45] requiring prior mapping of the environmental channel response, [66] utilizes a single on-board transceiver with a single transmitting antenna and two receiving antennas. This design is more compact, but still necessitated availing a dedicated battery to cope with the high power demand of radar.

4.4.2. Ultra-wideband and phased-array radio localization

Initially conceived for communication, UWB systems have been extended to incorporate ranging functionality [57]. Their precise timestamping and message scheduling supports TDOA (Time Difference of Arrival) and TWR (Two-Way Ranging) between tags and anchors [36], usable for localization. These modules are lightweight, consume less power, but are more suitable for indoor open spaces as clutter may lead to non-line-of-sight signal paths resulting in low accuracy.

For 3D position measurement, UWB requires precise installation of anchors in the environment limiting their usage to human accessible structured indoor environments. Nevertheless, indoor environments exhibit limited vertical clearance, a factor that results in poor height estimation accuracy relative to horizontal position accuracy. Additionally, UWB update rates scale inversely proportional to the number of tags tracked.

The first reviewed work [36] demonstrated an indoor 3D UWB positioning system for UAV localization that achieved ±0.20 m accuracy at 0.95 probability. The setup consisted of eight UWB nodes installed at different heights around the experimental volume. Each node run a decaWave ScenSor DWM1000 transceiver module. The estimated position is presented as a GNSS-pseudo-range message to emulate GNSS signals for ease of integration.

Fusion of UWB positioning and inertial positioning in an extended Kalman filter for UAV localization demonstrated in [57] achieved an accuracy of ±0.15 m at 0.95 probability using only four ultra-lightweight UbiSense UWB anchors. UWB positioning together with visual QR-codes placed in the environment provide inertial drift correction. This approach is highly inflexible since it requires not only installation of anchors in the environment, but also of QR-codes.

Following a strategy similar to [33,57] loosely coupled an inertial position, UWB position and 3D laser scanner position estimated at 100 Hz, 10 and 1 Hz respectively in a Kalman filter. The algorithm assumes knowledge of the start position and hovering at selected waypoints to enable the slow scanning process to take place. Despite intermittent motion, the proposed system achieved sub-centimetre accuracy when tested in simulation.

It is also possible to have UWB modules installed on mobile platforms as in [48] and [132] for air-to-ground cooperative localization. In [48], the UGV estimates its pose in the inertial frame using visual inertial odometry and shares it with the UAV via UWB communication channel. Then the UAV localizes itself in the inertial frame from its relative position to UGV and the shared UGV pose. In [132], the UGV localizes itself via DGPS (Differential Global Positioning System) while the UAV localizes itself from its relative position to the UGV tracked by UWB. The UGV is assumed to operate in a GNSS-enabled environment, while the UAV in a GNSS-denied environment.

PARS uses electronically steered radio waves for detection and ranging. [30] applied PARS and achieved GNSS-level positioning accuracy (6.86 m RMSE). However, unlike GNSS, PARS has a higher signal-to-noise ratio and supports encrypted communication. PARS consists of an on-board and ground module at a known location, in this case Radionor CRE2-189 and a 0.295 kg CRE2-144-M2-SMA module respectively. Phase difference of the signals received by the ground receiver is used to resolve azimuth, elevation and position of the vehicle. The authors assert that this aerial–ground radio combination can support up to 114 km line-of-sight ranging.

4.5. Above ground level estimation

This degree of freedom differentiates aerial robots and ground robots. AGL (Above Ground Level) measurements support not only take-off, cruise, landing flight phases, but also scale factor resolution in monocular vision as in [31,41,42] and optical flow algorithms.

Techniques for AGL estimation include altimeters, computer vision (stereo vision and optical flow), inertial odometry and beacons. Altimeters are the most commonly supported by sensors like ultrasonic, laser rangefinders, barometers and radar. Computer vision employs stereo and RGB-D cameras for AGL estimation. Inertial sensors double-integrate vertical IMU acceleration to obtain AGL. Noteworthy, laser rangefinders, ultrasonic, radar and vision sensors may generate false AGLs in presence

Table 10
AGL measurement systems.

Category	Sensor Modality	Pros and Cons	Sensors	Papers
Altimeter	Sonar	✓ Low SWaP ✗ Sensitive to temperature, humidity, atmospheric pressure ✗ Absorbed by materials like foam and fur ✗ Conical profile ✗ Limited range ✗ Low update rate	SRF08 UltraSonic Ranger (0.03–6 m, 5 V, 55°), HC-SR04 (0.02–4 m, 5 V, 15°, 40 Hz), LV-MaxSonar-EZ (0–6.45 m, 20 Hz)	[20,44,47,57,58,69,98,117]
	Barometer	✓ Low SWaP ✓ Absolute range measurement ✗ Low sensitivity to altitude changes ✗ Low update rate	MS5540 barometric altimeter (10–1100 mbar, 0.1 mbar resolution)	[30,31,42,51,72,117]
	Laser rangefinder	✓ High accuracy ✓ Point measurements ✓ High update rate ✓ Longer range ✗ Weather dependent	TeraRanger One (14 m, 6 m in sunlight, 8 g, 3°, 10–12 V) LiDAR Lite v3 and v2 (0–40 m, 22 g) Lightware SF10/A (25 m, 32 Hz, 35 g)	[14,37,48,64,70,88]
	Radar	✓ Longest sensor range ✓ Robust against weather conditions and illumination variations ✗ Relatively bulky ✗ Consumes relatively more power	Ultralight 24-GHz SENTIRE Radar (186 g, 0.1337 m × 0.0845 m × 0.0356 m, ±60°), smartmicro altimeter (0.5 m–500 m, 0.11 × 0.099 × 0.029 m, 350 g)	[54,66]
Computer vision	Stereo camera	✓ Rich information ✓ Situation awareness ✗ Limited depth measurement ✗ Illumination and weather dependent ✗ Requires unique features	n/a	[17]
	Stereo camera	✓ Resilient to illumination variations ✗ Limited depth range and resolution	Microsoft Kinect, Asus Xtion Pro live, Intel RealSense depth camera	[43]
	Motion capture system	✓ High update rate ✓ Highly accurate ✗ Limited range ✗ Expensive	OptiTrack	[71]

of ground obstacles, but barometers, motion capture systems and beacons are immune to this effect. Table 10 lists all AGL measurement techniques found in the reviewed literature.

Researchers have also fused complementary sensors to improve AGL estimation accuracy, robustness and reliability. Examples include IMU and barometer fusion in a complementary filter [133], IMU, 3D laser scanner and UWB fusion [33], IMU and barometer fusion [36], visual odometry fused with UAV and satellite image alignment using a deep convolutional network [46], IMU, ultrasonic and barometer fusion [86], fusion of IMU and visual motion [63], fusion of INS (Inertial Navigation System) and horizon profile matching [67], and fusion of IMU, barometer and laser rangefinder in an Extended Kalman Filter [19].

4.6. Environments

Environments can be classified as structured/unstructured, known/unknown/partially known, indoor/outdoor, 1D/2D/3D and static/dynamic. Each class offers different localization affordance. Structured environment may offer artificial markers, indoor environments may offer perspective lines, outdoor environments may offer texture etc. Localization requires environment-to-map association through sensors, which should be capable of perceiving localization affordance from the environment. Unfortunately, in an open world, environmental properties may vary over time, which adds to environmental complexity.

Environmental complexity could be a factor of obstacle density, obstacle dynamics, illumination intensity, spatial symmetry, signal attenuation, turbulence, structure and knowledge of the environment. Analysis of this complexity is a key input to the aerial platform and sensor selection process, and is one of the three factors, the others being mission complexity and human independence, that determined the level of autonomy of unmanned

systems [134]. Therefore, by the law of requisite variety, vehicle capability should match environmental complexity. For indoor, forested and urban canyons, multi-rotor vehicles are a more suitable choice because of their VTOL (Vertical Take-Off and Landing) capability and agility, while for outdoor and high-altitude flights, fixed-wing vehicles are better suited.

GNSS-denied environments explored in the reviewed literature include corridors [49,55], underground mines [79], urban canyons [23,132,135], forests [16,107] and outdoors [56].
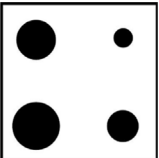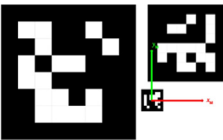
4.7. Take-off and landing

Take-off and landing are manoeuvres unique to aerial robots. Their criticality has earned them special treatment with dedicated control algorithms and articles like [100,101]. From Section 6, UAVs are characterized aerodynamically into ducted-fan, blimp, flapping-wing, fixed-wing, rotorcrafts and fixed-wing–rotorcraft hybrids, each with different take-off and landing requirements.

Fixed-wing aerial robots require a runway long enough for them to attain lift-off speed. Alternatively, catapult mechanisms or humans can launch the vehicles, but this necessitates deployment of a mid-air catch mechanism as opposed to landing. Unlike fixed-wing vehicles, ducted-fan, blimp and rotorcrafts exhibit VTOL capability eliminating the need for a runway or launch mechanism.

To land safely, aerial vehicles require the capability of identifying suitable landing surfaces. These surfaces may be static or dynamic, marked or unmarked. For marked surfaces, majority of markers are passive, but also active markers are applicable for example infrared lamps used in [99]. Characteristics of markers include uniqueness, orientation invariance, scalability with altitude, robustness against occlusion and illumination irregularities. Table 11 presents marker concepts found in the reviewed literature.

Table 11
Artificial landing pad markers.

Marker design	Properties	Papers
	• Non-scalable with altitude • Require full view of marker • Encodes position only	[98]
	• Scalable with altitude • Robust against partial occlusion • Encode position and height to a scale	[97]
	• Scalable with altitude • Robust against partial occlusion • Encodes position only	[136]
	• Scalable with altitude • Robust against partial occlusion • Encodes position and orientation	[105]
	• Non-scalable with altitude • Encodes position and orientation • Each marker is identifiable • Affected by partial occlusion	[14]
	• Scalable with altitude • Encode absolute position information and orientation • Each marker is identifiable • Robust against partial occlusion	[48,106]
	• Scalable with altitude • Robust against partial occlusion • Encodes position and orientation	[137]

5. Motion planning

Situatedness implies that robots are an intrinsic part of their operating environment. This obliges them to respect environmental geometric and kinematic constraints. This compliance is achieved by either manually programming robot task sequences or automatically generating task sequences compliant with such constraints. The former approach is tedious and time consuming, especially in high dimensional spaces, which motivated the latter known as motion planning.

Motion planning consists of path and trajectory planning, where the former generates an obstacle free path from a start to a goal configuration with no regard for vehicle dynamical constraints. The latter parametrizes a purely geometric path with time promoting it to a trajectory and enables consideration of differential and torque constraints on the generated path [138]. Since path planning and time scaling of the resulting path are performed sequentially, the resulting trajectory is typically not time-optimal. A time-optimal trajectory could be generated by planning directly in the state space [139].

Path planning may assume precise knowledge of all obstacles in the environment, which assumption is unrealistic when operating in an open world. Path planners founded on such an assumption are known as offline planners. Contrary to these are online planners, which account for incomplete obstacle information.

Paths are searched within partially or fully known workspaces. A workspace is a union of a closed set of obstacle configurations and an open set of free configurations. Configurations in the obstacle set involve collisions that violate geometric constraints, except in cases where such contact is part of the task, e.g. grasping or landing on an object, in which case the reachability structure becomes the closure of the free configuration. To simplify path planning, a robot geometry is equated to a particle. This simplification ignores geometric constraints, which are then incorporated through expansion of all obstacle boundaries by the radius of the robot silhouette. The resulting space with expanded obstacle boundaries is known as configuration space [140].

Path planning paradigms include sampling-based, combinatorial, potential field [141] and reward-based motion planners. Sampling planners probabilistically or deterministically sample the configuration space to build a data structure that captures the connectivity of the free configuration space. Deterministic sampling results in a regular data structure, which is resolution complete, while probabilistic sampling results in a random data structure, which is probabilistically complete [138]. Sampling planners belong to either PRM (Probabilistic Roadmap Method) multi-query planners or RRT (Rapidly Exploring Random Tree) single-query planners [22]. Combinatorial methods construct a roadmap from intersections of Voronoi roadmap segments. Potential field methods build a mapping from configuration to a potential, known as a potential function. Techniques like gradient descent can then be applied to this function, to guide a system downhill to a minimum. Reward-based planners select actions from a finite set of possible actions to maximize a future reward. As a result of the finite set of possible actions, this approach is suboptimal. A summary of differences between the three classical path planning paradigms is presented in Table 12.

No one path planning paradigm outperforms the others at all path planning scenarios [142], but among the four, only combinatorial methods exhibit completeness. Potential field methods are suitable for online path planning and provide measures for feedback control, but their gradient descent implementations are susceptible to local minima, leading to goal unreachability [80]. Unlike combinatorial and potential field methods, sampling-based methods apply to a wide range of path planning problems, thanks to their ability to scale to higher dimensional spaces and large problems with tractable computational costs [26,29], but generally produce poor quality paths. Looking at Table 6 and at Fig. 3, Combinatorial methods dominate among global path planners.

6. UAV classification

This section introduces a two-stage classification scheme for UAVs. The first stage classifies UAVs based on their aerodynamical configurations and the second stage classifies them based on MTOW (Maximum Take-Off Weight). Aerodynamical configurations include blimp, flapping-wing, fixed-wing, rotorcrafts, ducted-fan and combination thereof known as hybrid systems.
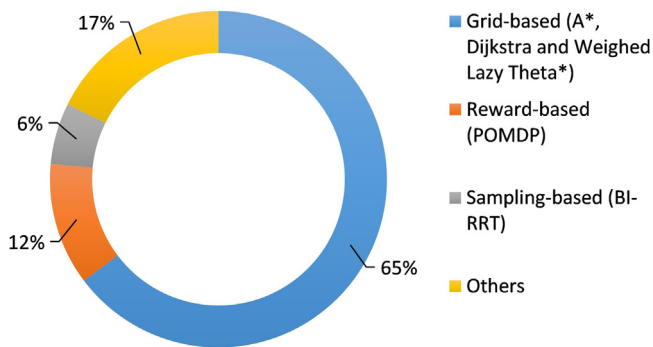
Blimps overcome gravity by regulating the density and pressure of the gas filling their hull making them lighter than ambient

Table 12

Differences between sampling, combinatorial and potential field path planning paradigms.

Sampling	Combinatorial	Potential fields
Builds a roadmap or tree	Builds a roadmap	Potential field function
No modelling of the obstacle configuration space	Models the obstacle configuration space	Models the obstacle configuration space
Probabilistically or resolution complete	Generally complete	No solution guarantees[a]
Applicable to higher dimensional configurations	Limited to lower dimensional configurations	Limited to lower dimensional configurations[b]
Online variants exist	Virtually always offline	Online capable
Complexity is independent of environmental complexity [143]	Complexity scales exponentially with problem dimensionality	Complexity scales exponentially with problem dimensionality

[a]Except in case of a navigation function or randomized potential planners. Despite completeness, both have a downside of requiring prior complete knowledge of the configuration space [144].
[b]With random walk augmentation as a way to overcome local minimum, this approach was able to plan in up to a 31 dimension configuration space [138].

Fig. 3. Global path planners.

Table 13

UAV classification.

Category	Maximum Take-off Weight (kg)
Nano	Up to 0.25
Micro	(0.25, 5.0]
Mini	(5.0, 30]
Small	(30, 100]
Lightweight	(100, 250]
Normal	(250, 5000]
Large	Above 5000

Table 14

Nano UAVs.

Brand	Specification
Black Hornet (for military) [10]	Helicopter, 0.016 kg, 25 min endurance, 0.12 m × 0.025 m, top speed 10 m/s, GPS controlled in outdoor environments
Nano Hummingbird (for military) [150]	Flapping-wings, 0.019 kg, wing-span 0.165 m, top speed 6.7 m/s, manually flown
Crazyflie 2.0 (for research) [71]	Quadrotor, 0.027 kg, 0.092 × 0.092 × 0.029 m
Parrot Mambo (for entertainment)	Quadrotor, 0.063 kg, 0.18 m × 0.18 m

air. They are capable of very long endurances, but operate at low speeds and are bulky [145]. Fixed-wing vehicles regulate their speed and the shape of their aerofoil wings to generate lift. They are capable of long endurance and high cruise speeds, but require continuous forward motion to stay airborne [129]. Rotorcrafts overcome gravity by regulating the rotational speed of their propeller blades. This enables them to achieve VTOL, hovering and high manoeuvrability, but consume more power. Flapping-wing vehicles mimic birds but are normally characterized by very lightweight chassis supported by relatively large wings.

The existing MTOW classification schemes as presented in [146] only support micro, mini, small, lightweight, normal and large vehicle classes. But the recent surge in the interest for nano vehicles both for civil and military applications rises the need for their inclusion as an independent class. Against this background, we propose a new MTOW classification scheme, presented in Table 13, which is an adaptation of the classification schemes from [147–149]. The weight range for the nano class has been inspired by the existing nano UAVs with examples presented in Table 14.

Table 15 gives an overview of aerial vehicles used to test the different navigation solutions from the reviewed literature. From an aerodynamical perspective, the presented vehicles fall under fixed-wing, rotorcrafts and ducted-fan classes only. As per the proposed MTOW classification scheme presented in Table 13, the vehicles presented herein fall under nano, micro, mini and small class.

7. Integrity of UAV navigation systems

UAV mishaps may result in costly property damage and loss of lives especially when operating in urban areas. Failure analysis conducted by US military on six normal-sized UAVs over a period of 17 years revealed that 57% of the failures were attributed to system design i.e. propulsion and flight control systems [151]. Navigation, which is the focus of this work, subsumes both propulsion and flight control systems making it a very critical part of any UAV.

Navigation is supported by sensors, actuators, algorithms and the environment all of which are potential fault sources. To ensure reliability, it is imperative to detect and eliminate faults before they compromise the system. In remotely piloted systems, human pilots may easily detect faults and avert impending failure. In autonomous systems, faults are either observed directly through sensors or indirectly through integrity monitoring algorithms.

Integrity monitors can be classified into model-based, signal processing-based, and knowledge-based approaches [152]. Model-based approaches derive and incorporate equations of motion into either state observers e.g. Luenberger observer [153] or state estimators like Kalman filters e.g. [154]. Signal processing-based approaches transform signals into representation for which the normal and faulty signals separate. Knowledge-based approaches derive a set of rules from expert knowledge capable of distinguishing known faulty from normal states.

A distribution is normally assumed on each state with normality defined to within a standard deviation threshold and any state outside this threshold is considered faulty. Mahalanobis

Table 15
Aerial vehicles applied in literature.

Type	Make	Class	Specs	Flight time (min)	Papers
Fixed-wing					
Fixed-wing	Prometheus	Mini	30 kg, 3.2 m wingspan	*n/a*	[54]
	PrecisionHawk Lancaster Rev IV	Micro	2.5 kg, 1.5 m wingspan	30–45	[61]
Multi-rotor					
Helicopter	ARTIS	Small	85 kg	*n/a*	[54]
	R-MAX	Small	66 kg, 3.115 m main rotor diameter	40	[58]
	Aerotech Cb-5000	*n/a*	1.8 m main rotor diameter	*n/a*	[102]
Quadcopter	In-house	Nano	0.045 kg, 0.15 m diagonal	8	[42]
	Crazyflie 2.0	Nano	0.027 kg, 0.092 × 0.092 × 0.029 m	*n/a*	[71]
	Pelican (AscTec)	Micro	1.4 kg	*n/a*	[34,74]
	Neo (AscTec)	Micro	2 kg	20	[25]
	Hummingbird (AscTec)	Micro	0.679 kg, 0.53 m diagonal	12–25	[72,97]
	Matrice 100 (DJI)	Micro	2.7−3.5 kg, 0.65 m diagonal	10	[17,109]
	Parrot AR.Drone	Micro	0.38 − 0.42 kg	5–12	[18,55,57,62,68,69,86,91,98]
	Parrot Bebop 2	*n/a*	*n/a*	*n/a*	[83]
	Mikrokopter L4-ME	*n/a*	*n/a*	5–6	[58]
	Mikrokopter XL	*n/a*	*n/a*	*n/a*	[20]
	In-house	Mini	8.5 kg, 0.5 × 0.5 m on the side	5	[35]
	In-house (DJI F450 frame)	Micro	1.15−3.0 kg, 0.55 m diagonal	*n/a*	[27,47,110]
	In-house	Micro	5 kg, 1.28 m diagonal	*n/a*	[50]
	In-house	Micro	3.2 kg, 0.62 × 0.62 × 0.4 m	12	[19]
	In-house	Micro	1.8 kg, 0.33 m diagonal	15	[29]
	Arducopter	*n/a*	*n/a*	*n/a*	[87]
	Pixhawk quadcopter	*n/a*	*n/a*	*n/a*	[76]
Hexacopter	In-house	Micro	1.6 kg	*n/a*	[14]
	In-house (DJI F550 frame)	Micro	3 kg, 0.55 m diagonal	*n/a*	[64]
	ARDEA	Micro	Coaxial, 2.65 kg, 0.68 × 0.68 × 0.3 m	*n/a*	[28]
Octocopter	Camflight BG-200 HL	*n/a*	Coaxial rotor, 1.4 m diameter	*n/a*	[30]
Single-rotor					
Ducted-fan	EASE	Micro	1.0 kg, 0.25 m duct diameter	<8	[116]

distance function is commonly applied for this check. The threshold value varies depending on the criticality of the system, task and environment. Therefore, different tasks and environments demand different RNP (Requirements of Navigation Performance). A set of metrics including PL (Protection Level), AL (Alert Limit), TTA (Time-to-Alert) and IR (Integrity Risk) has been adopted for integrity monitoring, but the thresholds are not standardized as of this writing.

Faults could be detected at sensor or state levels. The former associates each sensor with a fault detector, while the latter fuses sensor measurements together in an estimator and analyses the estimated state for faults. An example of the former is presented in [153], which is a model-based fault detector for an autonomous helicopter. For each sensor and its associated Luenberger observer, a residual is calculated and analysed for any anomalies. The results indicated successful detection of different faults, but also revealed an inverse relationship between drift magnitude and drift fault detectability.

It is also possible to combine mathematical models with data-driven models for fault detection. The work presented in [154] detected faults in a triaxial gyroscope mounted on a quadcopter using a neural network whose weights were updated by an EKF (Extended Kalman Filter). The algorithm successfully detected bias, step and triangular faults.

Others have combined model and knowledge-based approaches for fault detection, like the ANFIS (Adaptive Neuron Fuzzy Inference System) for position related fault detection in a UAV navigation system presented in [155]. The algorithm determines an F-indicator from R-Indicator and C-Indicator, which are functions of Kalman filter residual, and applies it to fuzzy rules for fault detection. A training dataset is continuously updated with every successful detection of a normal or a faulty state. Upon addition of a predefined number of new faulty samples, the neural network is retrained, which then updates the fuzzy rules. The approach is beneficial in terms of learning new rules to detect new faults, a feature that is missing in knowledge-based fault detectors.

Unlike the data-driven models in [154] and [155] that require training, [156] applied a non-parametric train-free data-driven approach that compares the current input to the previous normal inputs within a window of size n to determine if the current input is faulty. Before analysis, the input is filtered for noise reduction then applied to a Mahalanobis distance function to decide if it falls within the standard deviation threshold. This non-parametric, model free, unsupervised, online approach is applicable to different domains and data sources, and has been tested on a UAV, vacuum cleaning robot and electric power supply for fault detection.

In some cases, it is necessary not only to detect but also to eliminate faults. Fail-safe through hardware and software redundancy is demonstrated in [157]. Specifically, they demonstrated detection and recovery of actuator malfunction on a coaxial octorotor. With two rotors per arm, this provides a redundancy of one rotor per arm. Rotor failure is observed indirectly through Euler angles measured by an IMU. The detector Analyses residuals, discrepancy between sensor and non-linear sliding mode observer. Then the occurrence of a rotor failure is decided by a rule-based inference algorithm. Besides actuator redundancy, software redundancy is also implemented, where a different control law is executed during system recovery to account for changes in total thrust.

Each navigation technique requires a dedicated integrity analysis as these methods exhibit unique dynamics and hence failure modes. Of interest are vision-based navigation systems. Vision sensors have become an indispensable part of GNSS-denied navigation systems, but unlike GNSS, which exhibit fewer errors, in most cases one per component, visual navigation systems exhibit numerous simultaneous errors. This complicates the fault identification process. [158] proposed an integrity monitoring framework for a feature-based (ORB-SLAM2) visual localization system.

Table 16
Fault types and their likely causes. This table is an adaptation of the lists presented in [153,160].

Fault classification	Fault type		Cause
Hard failure	Point fault	Complete failure	Power disruption or communication blackout
Soft failure	Contextual fault	Bias fault	Current or voltage bias due to temperature change and or vibrations
	Collective fault	Drift fault	Internal temperature change or outdated calibration values
	Collective fault	Multiplicative fault	Environmental changes, component ageing
	Collective fault	Periodic fault	Environmental changes
	Collective fault	Outlier fault	Environmental changes

The framework applies an IPSOR (Iterative Parity Space Outlier Rejection) method that evaluates the distribution of weighed sum of squared residuals to determined whether an outlier measurement is present. This method relies on the assumption that inliers have a high precision. The iterative nature allows for elimination of multiple outliers, but not all outliers. It is assumed that at most a fault will ensue from the undetected outliers. After outlier rejection, protection levels in x, *y* and z directions are calculated and used to determine system integrity.

7.1. Fault modes in navigation systems

Navigation faults exhibit varying dynamic behaviours like ramp, bias, periodic oscillatory, step and sporadic. The five commonly tracked faults and their likely causes are presented in Table 16, which are classified into point, contextual and collective faults [159]. For point faults, a single value is sufficient to rule on occurrence of a fault, while for a contextual fault context and value are required. Ruling on collective faults require analysis of a sequence of values.

7.2. Existing challenges of integrity monitoring systems

Despite decades of research, there are still a number of challenges that need addressing. Here we provide a list of open challenges, this is not in any way comprehensive:

- Multiple fault detection. Most solutions in literature assume a single fault yet the complexity of navigation systems suggests a likelihood of multiple faults.
- Performance requirements. As of this writing, there are no standardized performance requirements for integrity monitoring in UAV navigation systems.
- Faults elimination techniques. With the exception of obvious cases like outlier rejection, fault elimination techniques are still lacking.
- Predictive fault monitoring. The existing fault detectors respond to occurrence of a fault, which in some cases might be too late for any correction measures. Therefore, raising a need for predictive fault detection.
- Computational complexity. Integration of integrity monitors into flight management systems may introduce competition for resources that may jeopardize system stability. Hence, the need for low computational complexity integrity monitoring-UAV navigation software architectures.

8. Technology readiness assessment of UAV navigation systems

This section uses TRLs (Technology Readiness Levels) adapted by ESA (European Space Agency) from the original TRLs developed by NASA and UAS (Unmanned Aerial System) adapted ATRA (Autonomy and Technology Readiness Assessment) [161] to determine the maturity of GNSS-independent navigation. This assessment serves as a progress evaluation step and a justification for efforts so far invested in addressing this navigation problem.

TRLs are a technology readiness assessment (TRA) framework consisting of nine levels [162].

Motivated by ATRA framework, we divide the nine TRLs into three clusters, research and development (levels 1–3), integration, testing and evaluation (levels 4–7), and production and deployment (levels 8–9). Levels 1–3 analyse the feasibility of the underlying theoretical premise. All reviewed research meets this feasibility check. Levels 4–7 tests and evaluates navigation technology against environmental complexity and performance metrics. Levels 8–9 look at deployment of the actual complete system in real scenarios. Table 17 presents the TRLs ratings of the full navigation solutions found in the reviewed literature, which indicates that the navigation technology is at TRL-6, interpreted as "Successful high fidelity prototype demonstrations in relevant environments" [161].

9. Future trends in the field of GNSS-independent UAV navigation

As revealed herein, navigation has not reached full technology maturity. This section highlights the likely future trends in sensing technology, algorithms, communication technology and simulation.

With the prevalence of off-the-shelf autopilots, it is safe to say that UAV flight controller and their associated structural designs have reached full technology maturity. So, the focus is now concentrated on perception, localization, motion planning and communication.

Towards perception, future research is expected to employ more advanced sensors like signal-of-opportunity sensors, event cameras and miniaturized radar. With advanced sensors also comes the need for advanced algorithms. Machine learning, active vision and other adaptive AI techniques are expected to become popular solutions for addressing sensor error modelling and semantic scene understanding. Last but not least, 5G communication technology is expected to become a key enabler for on-board data-driven navigation systems with its high volume real-time data streaming capability.

Going beyond TRL-6 demands deployment and testing of the proposed navigation solutions in their expected operating environments, a step that comes with great risks that might ensue from mishaps. Therefore, it is imperative to test out these systems on high fidelity simulators before deployment. Hence, the likely prevalence of high-fidelity UAV navigation simulators.

Looking at GNSS-based navigation systems that support launch-and-forget, GNSS-independent navigation solutions are soon to move towards such integrity, availability and continuity levels. Of course, this will be preceded by clear definition of levels of autonomy and standardization of performance requirements for GNSS-independent UAV navigation.

As indicated in Fig. 3, sampling-based path planners are the least applied despite their attractive properties, but the development of real-time and asymptotically optimal randomized sampling-based planners like real-time capable RRT-Connect [163] and asymptotically optimal RRG, PRM* and RRT* [164] suggests a likely prevalence in their applications.

Table 17
TRL rating of the full GNSS-denied navigation solutions from selected literature.

Paper	Perception	Solution description	TRL
[14]	Laser rangefinder, IMU and vision	On-board 2D SLAM, tested on a prototype in a partially known relevant environment	6
[15]	Vision, IMU	Visual-aided INS, tested in a simulated known environment (Software-in-the-loop)	5
[16]	Laser rangefinder, IMU and vision	On-board LiDAR 2D SLAM, tested on a prototype in an unknown cluttered relevant environment	6
[4]	Vision, IMU	3D visual SLAM, tested in a simulated unknown unstructured environment	5
[17]	Vision, IMU, sonar	On-board 3D visual SLAM, tested on a prototype in relevant environment	6
[18]	Vision, IMU	Off-board VIO, tested on a prototype in a known structured relevant environment	5
[19]	Laser rangefinder, IMU and vision	On-board 2D SLAM, tested on a prototype in a relevant environment	6
[20]	Vision, sonar, IMU	On-board 3D visual SLAM, tested on a prototype in a known structured relevant environment	6
[21]	Laser rangefinder, IMU and vision	On-board 3D SLAM, tested on a prototype in a relevant environment	6
[22]	Vision, sonar, IMU	Off-board 3D visual SLAM, tested on a prototype in a partially known unstructured environment	6
[23]	Laser rangefinder, IMU	Off-board 2D LiDAR SLAM, tested on a prototype in an unknown unstructured relevant environment	6
[24]	Vision and IMU	On-board 3D visual SLAM, tested on a prototype in a relevant environment	6
[25]	Vision and IMU	On-board 3D visual SLAM, tested on a prototype in a known relevant environment	6
[26]	Vision and IMU	On-board 3D visual SLAM, tested on a prototype in a partially known relevant environment	6
[27]	Laser rangefinder, IMU and vision	On-board 3D LiDAR SLAM, tested on a prototype in a partially known relevant environment	6
[28]	Vision and IMU	On-board 3D visual SLAM, tested on a prototype in a cluttered relevant environment	6
[29]	Vision and IMU	On-board 3D visual SLAM, tested on a prototype in a cluttered unknown relevant environment	6

10. Conclusion

This paper provides an account of GNSS-independent UAV navigation solutions proposed within the last decade. Of all reviewed works, full navigation solutions constituted only 16%. Majority of the reviewed works focused on localization, which corresponded to 62% followed by approach and landing, translational velocity estimation, obstacle avoidance, attitude estimation, mapping and motion planning at 11%, 4%, 3%, 2%, 1% and 1% respectively. The applied navigation modes included inertial, visual, LiDAR and radio navigation. Amongst the reviewed full navigation solutions, SLAM-based navigation dominated at 76% followed by visual inertial odometry and vision-aided inertial navigation systems at 18% and 6% respectively. With the reliability and high update rates of inertial systems, and rich representation of vision techniques, it is our conviction that inertial and optical hybridizations hold the key to successful GNSS-independent UAV navigation.

A technology readiness assessment of GNSS-independent navigation solutions indicated that the current solutions are of TRL-6, interpreted as "successful high fidelity prototype demonstrations in relevant environments". This observation together with the fact that the efforts targeted at full navigation solutions constituted only 16%, highlights the need for more and advanced research towards TRL-8 and TRL-9.

Flight control systems and structural design of UAVs reached full technology maturity and hence, have not been included in this study.

Declaration of competing interest

The authors declare that they have no known competing financial interests or personal relationships that could have appeared to influence the work reported in this paper.

References

[1] P. Radoglou-Grammatikis, P. Sarigiannidis, T. Lagkas, I. Moscholios, A compilation of UAV applications for precision agriculture, Comput. Netw. 172 (2020) 107148.

[2] H. Shakhatreh, A.H. Sawalmeh, A. Al-Fuqaha, Z. Dou, E. Almaita, I. Khalil, N.S. Othman, A. Khreishah, M. Guizani, Unmanned aerial vehicles (UAVs): A survey on civil applications and key research challenges, IEEE Access 7 (2019) 48572–48634.

[3] G. Schmidt, GPS based navigation systems in difficult environments, Gyroscopy Navig. 10 (2) (2019) 41–53.

[4] F. Vanegas, K.J. Gaston, J. Roberts, F. Gonzalez, A framework for UAV navigation and exploration in GPS-denied environments, in: 2019 IEEE Aerospace Conference, IEEE, 2019, pp. 1–6.

[5] R. Opromolla, G. Fasano, G. Rufino, M. Grassi, A. Savvaris, LIDAR-inertial integration for UAV localization and mapping in complex environments, in: 2016 International Conference on Unmanned Aircraft Systems (ICUAS), IEEE, 2016, pp. 649–656.

[6] G. Balamurugan, J. Valarmathi, V. Naidu, Survey on UAV navigation in GPS denied environments, in: 2016 International Conference on Signal Processing, Communication, Power and Embedded System (SCOPES), IEEE, 2016, pp. 198–204.

[7] L.M. Belmonte, R. Morales, A. Fernández-Caballero, Computer vision in autonomous unmanned aerial vehicles—a systematic mapping study, Appl. Sci. 9 (15) (2019) 3196.

[8] A. Al-Kaff, D. Martín, F. García, A. de la Escalera, J.M. Armingol, Survey of computer vision algorithms and applications for unmanned aerial vehicles, Expert Syst. Appl. 92 (2018) 447–463.

[9] Y. Lu, Z. Xue, G.-S. Xia, L. Zhang, A survey on vision-based UAV navigation, Geo-Spat. Inf. Sci. 21 (1) (2018) 21–32.

[10] G. Cai, J. Dias, L. Seneviratne, A survey of small-scale unmanned aerial vehicles: Recent advances and future development trends, Unmanned Syst. 2 (02) (2014) 175–199.

[11] S. Suzuki, Recent researches on innovative drone technologies in robotics field, Adv. Robot. 32 (19) (2018) 1008–1022.

[12] F. Kendoul, Survey of advances in guidance, navigation, and control of unmanned rotorcraft systems, J. Field Robotics 29 (2) (2012) 315–378.

[13] R. Siegwart, I.R. Nourbakhsh, D. Scaramuzza, Introduction to Autonomous Mobile Robots, MIT Press, 2011.

[14] Y. Bi, M. Lan, J. Li, K. Zhang, H. Qin, S. Lai, B.M. Chen, Robust autonomous flight and mission management for mavs in gps-denied environments, in: 2017 11th Asian Control Conference (ASCC), IEEE, 2017, pp. 67–72.

[15] A.R. Kuroswiski, N.M.F. de Oliveira, E.H. Shiguemori, Autonomous long-range navigation in GNSS-denied environment with low-cost UAV platform, in: 2018 Annual IEEE International Systems Conference (SysCon), IEEE, 2018, pp. 1–6.

[16] Y. Tang, Y. Hu, J. Cui, F. Liao, M. Lao, F. Lin, R.S. Teo, Vision-aided multi-UAV autonomous flocking in GPS-denied environment, IEEE Trans. Ind. Electron. 66 (1) (2018) 616–626.

[17] F. Valenti, D. Giaquinto, L. Musto, A. Zinelli, M. Bertozzi, A. Broggi, Enabling computer vision-based autonomous navigation for unmanned aerial vehicles in cluttered gps-denied environments, in: 2018 21st International Conference on Intelligent Transportation Systems (ITSC), IEEE, 2018, pp. 3886–3891.

[18] F. Vanegas Alvarez, F. Gonzalez, Uncertainty based online planning for UAV target finding in cluttered and GPS-denied environments, in: Proceedings of the 2016 IEEE Aerospace Conference, IEEE, 2016, pp. 706–714.

[19] C. Sampedro, A. Rodriguez-Ramos, H. Bavle, A. Carrio, P. de la Puente, P. Campoy, A fully-autonomous aerial robot for search and rescue applications in indoor environments using learning-based techniques, J. Intell. Robot. Syst. 95 (2) (2019) 601–627.

[20] R.C. Leishman, T.W. McLain, R.W. Beard, Relative navigation approach for vision-based aerial GPS-denied navigation, J. Intell. Robot. Syst. 74 (1–2) (2014) 97–111.

[21] M. Nieuwenhuisen, D. Droeschel, M. Beul, S. Behnke, Autonomous navigation for micro aerial vehicles in complex GNSS-denied environments, J. Intell. Robot. Syst. 84 (1–4) (2016) 199–216.

[22] Q. Li, D.-C. Li, Q.-f. Wu, L.-w. Tang, Y. Huo, Y.-x. Zhang, N. Cheng, Autonomous navigation and environment modeling for MAVs in 3-D enclosed industrial environments, Comput. Ind. 64 (9) (2013) 1161–1177.

[23] A. Bachrach, S. Prentice, R. He, N. Roy, RANGE–Robust autonomous navigation in GPS-denied environments, J. Field Robotics 28 (5) (2011) 644–666.

[24] K. Schmid, P. Lutz, T. Tomić, E. Mair, H. Hirschmüller, Autonomous vision-based micro air vehicle for indoor and outdoor navigation, J. Field Robotics 31 (4) (2014) 537–570.

[25] F.J. Perez-Grau, R. Ragel, F. Caballero, A. Viguria, A. Ollero, An architecture for robust UAV navigation in GPS-denied areas, J. Field Robotics 35 (1) (2018) 121–145.

[26] H. Oleynikova, C. Lanegger, Z. Taylor, M. Pantic, A. Millane, R. Siegwart, J. Nieto, An open-source system for vision-based micro-aerial vehicle mapping, planning, and flight in cluttered environments, J. Field Robotics 37 (4) (2020) 642–666.

[27] K. Mohta, M. Watterson, Y. Mulgaonkar, S. Liu, C. Qu, A. Makineni, K. Saulnier, K. Sun, A. Zhu, J. Delmerico, et al., Fast, autonomous flight in GPS-denied and cluttered environments, J. Field Robotics 35 (1) (2018) 101–120.

[28] P. Lutz, M.G. Müller, M. Maier, S. Stoneman, T. Tomić, I. von Bargen, M.J. Schuster, F. Steidle, A. Wedler, W. Stürzl, et al., ARDEA—An MAV with skills for future planetary missions, J. Field Robotics 37 (4) (2020) 515–551.

[29] Y. Lin, F. Gao, T. Qin, W. Gao, T. Liu, W. Wu, Z. Yang, S. Shen, Autonomous aerial navigation using monocular visual-inertial fusion, J. Field Robotics 35 (1) (2018) 23–51.

[30] K. Gryte, T.H. Bryne, S.M. Albrektsen, T.A. Johansen, Field test results of GNSS-denied inertial navigation aided by phased-array radio systems for UAVs, in: 2019 International Conference on Unmanned Aircraft Systems (ICUAS), IEEE, 2019, pp. 1398–1406.

[31] J. Duo, L. Zhao, Uav autonomous navigation system for gnss invalidation, in: 2017 36th Chinese Control Conference (CCC), IEEE, 2017, pp. 5777–5782.

[32] F. Causa, A.R. Vetrella, G. Fasano, D. Accardo, Multi-UAV formation geometries for cooperative navigation in GNSS-challenging environments, in: 2018 IEEE/ION Position, Location and Navigation Symposium (PLANS), IEEE, 2018, pp. 775–785.

[33] K. Li, C. Wang, S. Huang, G. Liang, X. Wu, Y. Liao, Self-positioning for UAV indoor navigation based on 3D laser scanner, UWB and INS, in: 2016 IEEE International Conference on Information and Automation (ICIA), IEEE, 2016, pp. 498–503.

[34] R. Mebarki, V. Lippiello, B. Siciliano, Nonlinear visual control of unmanned aerial vehicles in GPS-denied environments, IEEE Trans. Robot. 31 (4) (2015) 1004–1017.

[35] T. Pavlenko, M. Schütz, M. Vossiek, T. Walter, S. Montenegro, Wireless local positioning system for controlled UAV landing in GNSS-denied environment, in: 2019 IEEE 5th International Workshop on Metrology for AeroSpace (MetroAeroSpace), IEEE, 2019, pp. 171–175.

[36] J. Tiemann, F. Schweikowski, C. Wietfeld, Design of an UWB indoor-positioning system for UAV navigation in GNSS-denied environments, in: 2015 International Conference on Indoor Positioning and Indoor Navigation (IPIN), IEEE, 2015, pp. 1–7.

[37] J. Unicomb, L. Dantanarayana, J. Arukgoda, R. Ranasinghe, G. Dissanayake, T. Furukawa, Distance function based 6dof localization for unmanned aerial vehicles in gps denied environments, in: 2017 IEEE/RSJ International Conference on Intelligent Robots and Systems (IROS), IEEE, 2017, pp. 5292–5297.

[38] H. Xie, K.H. Low, Z. He, Adaptive visual servoing of unmanned aerial vehicles in GPS-denied environments, IEEE/ASME Trans. Mechatronics 22 (6) (2017) 2554–2563.

[39] S. Zahran, A. Moussa, N. El-Sheimy, Enhanced UAV navigation in GNSS denied environment using repeated dynamics pattern recognition, in: 2018 IEEE/ION Position, Location and Navigation Symposium (PLANS), IEEE, 2018, pp. 1135–1142.

[40] L. Zhang, M. Ye, B.D. Anderson, P. Sarunic, H. Hmam, Cooperative localisation of UAVs in a GPS-denied environment using bearing measurements, in: 2016 IEEE 55th Conference on Decision and Control (CDC), IEEE, 2016, pp. 4320–4326.

[41] C. Wang, T. Wang, J. Liang, Y. Chen, Y. Zhang, C. Wang, Monocular visual SLAM for small UAVs in GPS-denied environments, in: 2012 IEEE International Conference on Robotics and Biomimetics (ROBIO), IEEE, 2012, pp. 896–901.

[42] X. Zhang, B. Xian, B. Zhao, Y. Zhang, Autonomous flight control of a nano quadrotor helicopter in a GPS-denied environment using on-board vision, IEEE Trans. Ind. Electron. 62 (10) (2015) 6392–6403.

[43] A.R. Vetrella, A. Savvaris, G. Fasano, D. Accardo, RGB-D camera-based quadrotor navigation in GPS-denied and low light environments using known 3D markers, in: 2015 International Conference on Unmanned Aircraft Systems (ICUAS), IEEE, 2015, pp. 185–192.

[44] A. Al-Radaideh, L. Sun, Observability analysis and Bayesian filtering for self-localization of a tethered multicopter in GPS-denied environments, in: 2019 International Conference on Unmanned Aircraft Systems (ICUAS), IEEE, 2019, pp. 1041–1047.

[45] P. DeFranco, J.D. Mackie, M. Morin, K.F. Warnick, Bio-inspired electro-magnetic orientation for UAVs in a GPS-denied environment using MIMO channel sounding, IEEE Trans. Antennas and Propagation 62 (10) (2014) 5250–5259.

[46] H. Goforth, S. Lucey, GPS-denied UAV localization using pre-existing satellite imagery, in: 2019 International Conference on Robotics and Automation (ICRA), IEEE, 2019, pp. 2974–2980.

[47] C. Hui, C. Yousheng, W.W. Shing, Trajectory tracking and formation flight of autonomous UAVs in GPS-denied environments using onboard sensing, in: Proceedings of 2014 IEEE Chinese Guidance, Navigation and Control Conference, IEEE, 2014, pp. 2639–2645.

[48] T.-M. Nguyen, T.H. Nguyen, M. Cao, Z. Qiu, L. Xie, Integrated uwb-vision approach for autonomous docking of uavs in gps-denied environments, in: 2019 International Conference on Robotics and Automation (ICRA), IEEE, 2019, pp. 9603–9609.

[49] R.P. Padhy, F. Xia, S.K. Choudhury, P.K. Sa, S. Bakshi, Monocular vision aided autonomous UAV navigation in indoor corridor environments, IEEE Trans. Sustain. Comput. 4 (1) (2018) 96–108.

[50] H. Qin, Y. Bi, K.Z. Ang, K. Wang, J. Li, M. Lan, M. Shan, F. Lin, A stereo and rotating laser framework for UAV navigation in GPS denied environment, in: IECON 2016-42nd Annual Conference of the IEEE Industrial Electronics Society, IEEE, 2016, pp. 6061–6066.

[51] M. Shan, F. Wang, F. Lin, Z. Gao, Y.Z. Tang, B.M. Chen, Google map aided visual navigation for UAVs in GPS-denied environment, in: 2015 IEEE International Conference on Robotics and Biomimetics (ROBIO), IEEE, 2015, pp. 114–119.

[52] M. Suresh, D. Ghose, Group coordination and path replan tactics in gps denied environments, in: 2016 International Conference on Unmanned Aircraft Systems (ICUAS), IEEE, 2016, pp. 31–39.

[53] S. Rady, A. Kandil, E. Badreddin, A hybrid localization approach for uav in gps denied areas, in: 2011 IEEE/SICE International Symposium on System Integration (SII), IEEE, 2011, pp. 1269–1274.

[54] F. Andert, N. Ammann, S. Krause, S. Lorenz, D. Bratanov, L. Mejias, Optical-aided aircraft navigation using decoupled visual SLAM with range sensor augmentation, J. Intell. Robot. Syst. 88 (2–4) (2017) 547–565.

[55] F. de Babo Martins, L.F. Teixeira, R. Nóbrega, Visual-inertial based autonomous navigation, in: Robot 2015: Second Iberian Robotics Conference, Springer, 2016, pp. 561–572.

[56] F. Andert, J. Dittrich, S. Batzdorfer, M. Becker, U. Bestmann, P. Hecker, A flight state estimator that combines stereo-vision, INS, and satellite pseudo-ranges, in: Advances in Aerospace Guidance, Navigation and Control, Springer, 2013, pp. 277–296.

[57] A. Benini, A. Mancini, S. Longhi, An imu/uwb/vision-based extended kalman filter for mini-uav localization in indoor environment using 802.15. 4a wireless sensor network, J. Intell. Robot. Syst. 70 (1–4) (2013) 461–476.

[58] J. Chudoba, M. Kulich, M. Saska, T. Báča, L. Přeučil, Exploration and mapping technique suited for visual-features based localization of mavs, J. Intell. Robot. Syst. 84 (1–4) (2016) 351–369.

[59] S.J. Dumble, P.W. Gibbens, Airborne vision-aided navigation using road intersection features, J. Intell. Robot. Syst. 78 (2) (2015) 185–204.

[60] H. Yu, F. Zhang, P. Huang, CSLAM and GPS based navigation for multi-UAV cooperative transportation system, in: International Conference on Intelligent Robotics and Applications, Springer, 2019, pp. 315–326.

[61] M. Warren, M. Paton, K. MacTavish, A.P. Schoellig, T.D. Barfoot, Towards visual teach and repeat for GPS-denied flight of a fixed-wing UAV, in: Field and Service Robotics, Springer, 2018, pp. 481–498.

[62] S. Wang, T. Hu, ROS-gazebo supported platform for tag-in-loop indoor localization of quadrocopter, in: W. Chen, K. Hosoda, E. Menegatti, M. Shimizu, H. Wang (Eds.), Intelligent Autonomous Systems 14, Springer International Publishing, Cham, 2017, pp. 185–197.

[63] C.-L. Wang, T.-M. Wang, J.-H. Liang, Y.-C. Zhang, Y. Zhou, Bearing-only visual SLAM for small unmanned aerial vehicles in GPS-denied environments, Int. J. Autom. Comput. 10 (5) (2013) 387–396.

[64] V. Walter, T. Novák, M. Saska, Self-localization of unmanned aerial vehicles based on optical flow in onboard camera images, in: J. Mazal (Ed.), Modelling and Simulation for Autonomous Systems, Springer International Publishing, Cham, 2018, pp. 106–132.

[65] A. Volkova, P.W. Gibbens, More robust features for adaptive visual navigation of UAVs in mixed environments, J. Intell. Robot. Syst. 90 (1–2) (2018) 171–187.

[66] A.F. Scannapieco, A. Renga, G. Fasano, A. Moccia, Experimental analysis of radar odometry by commercial ultralight radar sensor for miniaturized UAS, J. Intell. Robot. Syst. 90 (3–4) (2018) 485–503.

[67] S.J. Dumble, P.W. Gibbens, Efficient terrain-aided visual horizon based attitude estimation and localization, J. Intell. Robot. Syst. 78 (2) (2015) 205–221.

[68] T. Nguyen, G.K. Mann, R.G. Gosine, A. Vardy, Appearance-based visual-teach-and-repeat navigation technique for micro aerial vehicle, J. Intell. Robot. Syst. 84 (1–4) (2016) 217–240.

[69] E. López, R. Barea, A. Gómez, A. Saltos, L.M. Bergasa, E.J. Molinos, A. Nemra, Indoor SLAM for micro aerial vehicles using visual and laser sensor fusion, in: Robot 2015: Second Iberian Robotics Conference, Springer, 2016, pp. 531–542.

[70] W. Liu, D. Zou, D. Sartori, L. Pei, W. Yu, An image-guided autonomous navigation system for multi-rotor UAVs, in: China Satellite Navigation Conference, Springer, 2019, pp. 513–526.

[71] X.W. Leong, H. Hesse, Vision-based navigation for control of micro aerial vehicles, in: IRC-SET 2018, Springer, 2019, pp. 413–427.

[72] F. Kendoul, K. Nonami, I. Fantoni, R. Lozano, An adaptive vision-based autopilot for mini flying machines guidance, navigation and control, Auton. Robots 27 (3) (2009) 165.

[73] X. Liu, X. Tao, Y. Duan, N. Ge, Visual information assisted UAV positioning using priori remote-sensing information, Multimedia Tools Appl. 77 (11) (2018) 14461–14480.

[74] J. Marzat, S. Bertrand, A. Eudes, M. Sanfourche, J. Moras, Reactive MPC for autonomous MAV navigation in indoor cluttered environments: Flight experiments, IFAC-PapersOnLine 50 (1) (2017) 15996–16002.

[75] A.K. Nasir, A. Hsino, H. Roth, K. Hartmann, Aerial robot localization using ground robot tracking–towards cooperative SLAM, IFAC Proc. Vol. 46 (19) (2013) 313–318.

[76] S. Yang, S.A. Scherer, X. Yi, A. Zell, Multi-camera visual SLAM for autonomous navigation of micro aerial vehicles, Robot. Auton. Syst. 93 (2017) 116–134.

[77] X. Wan, J. Liu, H. Yan, G.L. Morgan, Illumination-invariant image matching for autonomous UAV localisation based on optical sensing, ISPRS J. Photogramm. Remote Sens. 119 (2016) 198–213.

[78] C. Troiani, A. Martinelli, C. Laugier, D. Scaramuzza, Low computational-complexity algorithms for vision-aided inertial navigation of micro aerial vehicles, Robot. Auton. Syst. 69 (2015) 80–97.

[79] S.S. Mansouri, C. Kanellakis, D. Kominiak, G. Nikolakopoulos, Deploying MAVs for autonomous navigation in dark underground mine environments, Robot. Auton. Syst. 126 (2020) 103472.

[80] T.T. Mac, C. Copot, R. De Keyser, C.M. Ionescu, The development of an autonomous navigation system with optimal control of an UAV in partly unknown indoor environment, Mechatronics 49 (2018) 187–196.

[81] Y. Li, Y. Wang, D. Wang, Multiple RGB-D sensor-based 3-D reconstruction and localization of indoor environment for mini MAV, Comput. Electr. Eng. 70 (2018) 509–524.

[82] M. Alnuaimi, M.G. Perhinschi, Alternative approaches for UAV dead reckoning based on the immunity paradigm, Aerosp. Sci. Technol. 98 (2020) 105742.

[83] A. Haque, A. Elsaharti, T. Elderini, M.A. Elsaharty, J. Neubert, UAV autonomous localization using macro-features matching with a CAD model, Sensors 20 (3) (2020) 743.

[84] E. Hong, J. Lim, Visual-inertial odometry with robust initialization and online scale estimation, Sensors 18 (12) (2018) 4287.

[85] D.O. Nitti, F. Bovenga, M.T. Chiaradia, M. Greco, G. Pinelli, Feasibility of using synthetic aperture radar to aid UAV navigation, Sensors 15 (8) (2015) 18334–18359.

[86] F. Vanegas, F. Gonzalez, Enabling UAV navigation with sensor and environmental uncertainty in cluttered and GPS-denied environments, Sensors 16 (5) (2016) 666.

[87] J. Li-Chee-Ming, C. Armenakis, UAV navigation system using line-based sensor pose estimation, Geo-Spat. Inf. Sci. 21 (1) (2018) 2–11.

[88] E.T. Dill, M. Uijt de Haag, 3D multi-copter navigation and mapping using GPS, inertial, and LiDAR, Navig.: J. Inst. Navig. 63 (2) (2016) 205–220.

[89] S. Zahran, A. Moussa, N. El-Sheimy, A.B. Sesay, Hybrid machine learning VDM for UAVs in GNSS-denied environment, Navig.: J. Inst. Navig. 65 (3) (2018) 477–492.

[90] S. Weiss, D. Scaramuzza, R. Siegwart, Monocular-SLAM–based navigation for autonomous micro helicopters in GPS-denied environments, J. Field Robotics 28 (6) (2011) 854–874.

[91] A.L. Majdik, D. Verda, Y. Albers-Schoenberg, D. Scaramuzza, Air-ground matching: Appearance-based GPS-denied urban localization of micro aerial vehicles, J. Field Robotics 32 (7) (2015) 1015–1039.

[92] K. Lee, J.M. Kriesel, N. Gat, Autonomous airborne video-aided navigation, Navigation 57 (3) (2010) 163–173.

[93] Z. Hou, J. Qi, M. Wang, Fusing optical flow and inertial data for UAV motion estimation in GPS-denied environment, in: 2019 Chinese Control Conference (CCC), IEEE, 2019, pp. 7791–7796.

[94] R. Mebarki, V. Lippiello, Image moments-based velocity estimation of UAVs in GPS denied environments, in: 2014 IEEE International Symposium on Safety, Security, and Rescue Robotics (2014), IEEE, 2014, pp. 1–6.

[95] Y. Zhang, T. Wang, Z. Cai, Y. Wang, Z. You, The use of optical flow for UAV motion estimation in indoor environment, in: 2016 IEEE Chinese Guidance, Navigation and Control Conference (CGNCC), IEEE, 2016, pp. 785–790.

[96] R. Mebarki, J. Cacace, V. Lippiello, Velocity estimation of an UAV using visual and IMU data in a GPS-denied environment, in: 2013 IEEE International Symposium on Safety, Security, and Rescue Robotics (SSRR), IEEE, 2013, pp. 1–6.

[97] S. Lange, N. Sunderhauf, P. Protzel, A vision based onboard approach for landing and position control of an autonomous multirotor UAV in GPS-denied environments, in: 2009 International Conference on Advanced Robotics, IEEE, 2009, pp. 1–6.

[98] S. Dotenco, F. Gallwitz, E. Angelopoulou, Autonomous approach and landing for a low-cost quadrotor using monocular cameras, in: European Conference on Computer Vision, Springer, 2014, pp. 209–222.

[99] Y. Gui, P. Guo, H. Zhang, Z. Lei, X. Zhou, J. Du, Q. Yu, Airborne vision-based navigation method for UAV accuracy landing using infrared lamps, J. Intell. Robot. Syst. 72 (2) (2013) 197–218.

[100] D. Zhang, X. Wang, Autonomous landing control of fixed-wing uavs: from theory to field experiment, J. Intell. Robot. Syst. 88 (2–4) (2017) 619–634.

[101] C. Brooks, C. Goulet, M. Galloway, Toward indoor autonomous flight using a multi-rotor vehicle, in: Information Technology: New Generations, Springer, 2016, pp. 1145–1155.

[102] F. Alarcon, D. Santamaria, A. Viguria, UAV helicopter relative state estimation for autonomous landing on moving platforms in a GPS-denied scenario, IFAC-PapersOnLine 48 (9) (2015) 37–42.

[103] M.K. Al-Sharman, B.J. Emran, M.A. Jaradat, H. Najjaran, R. Al-Husari, Y. Zweiri, Precision landing using an adaptive fuzzy multi-sensor data fusion architecture, Appl. Soft Comput. 69 (2018) 149–164.

[104] A. Borowczyk, D.-T. Nguyen, A. Phu-Van Nguyen, D.Q. Nguyen, D. Saussié, J. Le Ny, Autonomous landing of a multirotor micro air vehicle on a high velocity ground vehicle, Ifac-Papersonline 50 (1) (2017) 10488–10494.

[105] J. Garcia-Pulido, G. Pajares, S. Dormido, J.M. de la Cruz, Recognition of a landing platform for unmanned aerial vehicles by using computer vision-based techniques, Expert Syst. Appl. 76 (2017) 152–165.

[106] M. Bhargavapuri, A.K. Shastry, H. Sinha, S.R. Sahoo, M. Kothari, Vision-based autonomous tracking and landing of a fully-actuated rotorcraft, Control Eng. Pract. 89 (2019) 113–129.

[107] F. Liao, S. Lai, Y. Hu, J. Cui, J.L. Wang, R. Teo, F. Lin, 3D motion planning for UAVs in GPS-denied unknown forest environment, in: 2016 IEEE Intelligent Vehicles Symposium (IV), IEEE, 2016, pp. 246–251.

[108] J. Zhao, X. Ma, Q. Fu, C. Hu, S. Yue, An LGMD based competitive collision avoidance strategy for UAV, in: IFIP International Conference on Artificial Intelligence Applications and Innovations, Springer, 2019, pp. 80–91.

[109] L. Zheng, P. Zhang, J. Tan, F. Li, The obstacle detection method of uav based on 2D lidar, IEEE Access 7 (2019) 163437–163448.

[110] H.D. Escobar-Alvarez, N. Johnson, T. Hebble, K. Klingebiel, S.A. Quintero, J. Regenstein, N.A. Browning, R-ADVANCE: Rapid adaptive prediction for vision-based autonomous navigation, control, and evasion, J. Field Robotics 35 (1) (2018) 91–100.

[111] A. Shabayek, C. Demonceaux, O. Morel, D. Fofi, Vision based UAV attitude estimation: Progress and insights, J. Intell. Robot. Syst. 65 (2012) 295–308, http://dx.doi.org/10.1007/s10846-011-9588-y.

[112] H.G. De Marina, F. Espinosa, C. Santos, Adaptive UAV attitude estimation employing unscented Kalman filter, FOAM and low-cost MEMS sensors, Sensors 12 (7) (2012) 9566–9585.

[113] S. Weiss, M. Achtelik, L. Kneip, D. Scaramuzza, R. Siegwart, Intuitive 3D maps for MAV terrain exploration and obstacle avoidance, J. Intell. Robot. Syst. 61 (1–4) (2011) 473–493.

[114] J. Vautherin, S. Rutishauser, K. Schneider-Zapp, H.F. Choi, V. Chovancova, A. Glass, C. Strecha, Photogrammetric accuracy and modeling of rolling shutter cameras, ISPRS Ann. Photogramm. Remote Sens. Spat. Inf. Sci. 3 (3) (2016).

[115] H. Qin, Z. Meng, W. Meng, X. Chen, H. Sun, F. Lin, M.H. Ang, Autonomous exploration and mapping system using heterogeneous UAVs and UGVs in GPS-denied environments, IEEE Trans. Veh. Technol. 68 (2) (2019) 1339–1350.

[116] G. Chowdhary, E.N. Johnson, D. Magree, A. Wu, A. Shein, GPS-denied indoor and outdoor monocular vision aided navigation and control of unmanned aircraft, J. Field Robotics 30 (3) (2013) 415–438.

[117] C. Shang, L. Cheng, Q. Yu, X. Wang, R. Peng, Y. Chen, H. Wu, Q. Zhu, Micro aerial vehicle autonomous flight control in tunnel environment, in: 2017 9th International Conference on Modelling, Identification and Control (ICMIC), IEEE, 2017, pp. 93–98.

[118] D. Scaramuzza, Z. Zhang, Visual-inertial odometry of aerial robots, 2019, arXiv preprint arXiv:1906.03289.

[119] D. Eynard, P. Vasseur, C. Demonceaux, V. Frémont, UAV altitude estimation by mixed stereoscopic vision, in: 2010 IEEE/RSJ International Conference on Intelligent Robots and Systems, IEEE, 2010, pp. 646–651.

[120] J. Madeiras, C. Cardeira, P. Oliveira, Vision-aided complementary filter for attitude and position estimation: Design, analysis and experimental validation, IFAC-PapersOnLine 52 (12) (2019) 388–393.

[121] R. Murphy, An Introduction to AI Robotics (Intelligent Robotics and Autonomous Agents), in: A Bradford Book, 2000.

[122] S. Thrun, W. Burgard, D. Fox, Probabilistic Robotics, MIT Press, 2005.

[123] S.M. Siam, H. Zhang, Fast-SeqSLAM: A fast appearance based place recognition algorithm, in: 2017 IEEE International Conference on Robotics and Automation (ICRA), IEEE, 2017, pp. 5702–5708.

[124] Q. Wang, M. Fu, Z. Deng, H. Ma, A comparison of loosely-coupled mode and tightly-coupled mode for INS/VMS, in: 2012 American Control Conference (ACC), IEEE, 2012, pp. 6346–6351.

[125] J. Engel, T. Schöps, D. Cremers, LSD-SLAM: Large-scale direct monocular SLAM, in: European Conference on Computer Vision, Springer, 2014, pp. 834–849.

[126] N. Yang, R. Wang, D. Cremers, Feature-based or direct: An evaluation of monocular visual odometry, 2017, pp. 1–12, arXiv preprint arXiv:1705.04300.

[127] C. Forster, Z. Zhang, M. Gassner, M. Werlberger, D. Scaramuzza, SVO: Semidirect visual odometry for monocular and multicamera systems, IEEE Trans. Robot. 33 (2) (2016) 249–265.

[128] R. Szeliski, Computer Vision: Algorithms and Applications, Springer Science & Business Media, 2010.

[129] Y. Li, M. Scanavino, E. Capello, F. Dabbene, G. Guglieri, A. Vilardi, A novel distributed architecture for UAV indoor navigation, Transp. Res. Procedia 35 (2018) 13–22.

[130] Y. Song, B. Xian, Y. Zhang, X. Jiang, X. Zhang, Towards autonomous control of quadrotor unmanned aerial vehicles in a GPS-denied urban area via laser ranger finder, Optik 126 (23) (2015) 3877–3882.

[131] D. Chen, G.X. Gao, Probabilistic graphical fusion of LiDAR, GPS, and 3D building maps for urban UAV navigation, Navigation 66 (1) (2019) 151–168.

[132] V.O. Sivaneri, J.N. Gross, UGV-to-UAV cooperative ranging for robust navigation in GNSS-challenged environments, Aerosp. Sci. Technol. 71 (2017) 245–255.

[133] S. Wei, G. Dan, H. Chen, Altitude data fusion utilising differential measurement and complementary filter, IET Sci. Meas. Technol. 10 (8) (2016) 874–879.

[134] H.-M. Huang, K. Pavek, J. Albus, E. Messina, Autonomy levels for unmanned systems (ALFUS) framework: An update, in: Unmanned Ground Vehicle Technology VII, Vol. 5804, International Society for Optics and Photonics, 2005, pp. 439–448.

[135] G. Zhang, L.-T. Hsu, Intelligent GNSS/INS integrated navigation system for a commercial UAV flight control system, Aerosp. Sci. Technol. 80 (2018) 368–380.

[136] L.R.G. Carrillo, E. Rondon, A. Sanchez, A. Dzul, R. Lozano, Position control of a quad-rotor UAV using vision, IFAC Proc. Vol. 43 (15) (2010) 31–36.

[137] T.S. Richardson, C.G. Jones, A. Likhoded, E. Sparks, A. Jordan, I. Cowling, S. Willcox, Automated vision-based recovery of a rotary wing unmanned aerial vehicle onto a moving platform, J. Field Robotics 30 (5) (2013) 667–684.

[138] S.M. LaValle, Planning Algorithms, Cambridge University Press, 2006.

[139] K.M. Lynch, F.C. Park, Modern Robotics: Mechanics, Planning, and Control, Cambridge University Press, 2017.

[140] N. Correll, Introduction to Autonomous Robots, 2016.

[141] B. Siciliano, O. Khatib, Springer Handbook of Robotics, Springer, 2016.

[142] S.M. LaValle, Rapidly-exploring random trees: A new tool for path planning.

[143] A. Gasparetto, P. Boscariol, A. Lanzutti, R. Vidoni, Path planning and trajectory planning algorithms: A general overview, in: Motion and Operation Planning of Robotic Systems, Springer, 2015, pp. 3–27.

[144] H.M. Choset, S. Hutchinson, K.M. Lynch, G. Kantor, W. Burgard, L.E. Kavraki, S. Thrun, R.C. Arkin, Principles of Robot Motion: Theory, Algorithms, and Implementation, MIT Press, 2005.

[145] K. Nonami, F. Kendoul, S. Suzuki, W. Wang, D. Nakazawa, Autonomous Flying Robots: Unmanned Aerial Vehicles and Micro Aerial Vehicles, Springer Science & Business Media, 2010.

[146] K. Dalamagkidis, Classification of uavs, in: Handbook of Unmanned Aerial Vehicles, 2015, pp. 83–91.

[147] P. van Blyenburgh, UAV systems: global review, in: Conference, Amsterdam, the Netherlands, 2006.

[148] K. Dalamagkidis, K.P. Valavanis, L.A. Piegl, On Integrating Unmanned Aircraft Systems Into the National Airspace System: Issues, Challenges, Operational Restrictions, Certification, and Recommendations, Vol. 54, springer science & Business Media, 2011.

[149] G. Cai, B.M. Chen, T.H. Lee, Unmanned Rotorcraft Systems, Springer Science & Business Media, 2011.

[150] M. Keennon, K. Klingebiel, H. Won, Development of the nano hummingbird: A tailless flapping wing micro air vehicle, in: 50th AIAA Aerospace Sciences Meeting Including the New Horizons Forum and Aerospace Exposition, 2012, p. 588.

[151] S.A. Cambone, K. Krieg, P. Pace, W. Linton, Unmanned Aircraft Systems Roadmap 2005–2030, Vol. 8, Office of the Secretary of Defense, 2005, pp. 4–15.

[152] X. Qi, D. Theilliol, J. Qi, Y. Zhang, J. Han, D. Song, L. Wang, Y. Xia, Fault diagnosis and fault tolerant control methods for manned and unmanned helicopters: a literature review, in: 2013 Conference on Control and Fault-Tolerant Systems (SysTol), IEEE, 2013, pp. 132–139.

[153] G. Heredia, A. Ollero, R. Mahtani, M. Béjar, V. Remuß, M. Musial, Detection of sensor faults in autonomous helicopters, in: Proceedings of the 2005 IEEE International Conference on Robotics and Automation, IEEE, 2005, pp. 2229–2234.

[154] P. Aboutalebi, A. Abbaspour, P. Forouzannezhad, A. Sargolzaei, A novel sensor fault detection in an unmanned quadrotor based on adaptive neural observer, J. Intell. Robot. Syst. 90 (3) (2018) 473–484.

[155] R. Sun, Q. Cheng, G. Wang, W.Y. Ochieng, A novel online data-driven algorithm for detecting UAV navigation sensor faults, Sensors 17 (10) (2017) 2243.

[156] E. Khalastchi, M. Kalech, G.A. Kaminka, R. Lin, Online data-driven anomaly detection in autonomous robots, Knowl. Inf. Syst. 43 (3) (2015) 657–688.

[157] M. Saied, B. Lussier, I. Fantoni, C. Francis, H. Shraim, G. Sanahuja, Fault diagnosis and fault-tolerant control strategy for rotor failure in an octorotor, in: 2015 IEEE International Conference on Robotics and Automation (ICRA), IEEE, 2015, pp. 5266–5271.

[158] C. Li, S.L. Waslander, Visual measurement integrity monitoring for uav localization, in: 2019 IEEE International Symposium on Safety, Security, and Rescue Robotics (SSRR), IEEE, 2019, pp. 22–29.

[159] V. Chandola, A. Banerjee, V. Kumar, Anomaly detection: A survey, ACM Comput. Surv. 41 (3) (2009) 1–58.

[160] Y.H. Gao, D. Zhao, Y.B. Li, UAV sensor fault diagnosis technology: A survey, in: Applied Mechanics and Materials, Vol. 220, Trans Tech Publ, 2012, pp. 1833–1837.

[161] F. Kendoul, Towards a unified framework for uas autonomy and technology readiness assessment (atra), in: Autonomous Control Systems and Vehicles, Springer, 2013, pp. 55–71.

[162] J.C. Mankins, Technology readiness assessments: A retrospective, Acta Astronaut. 65 (9–10) (2009) 1216–1223.

[163] J.J. Kuffner, S.M. LaValle, RRT-connect: An efficient approach to single-query path planning, in: Proceedings 2000 ICRA. Millennium Conference. IEEE International Conference on Robotics and Automation. Symposia Proceedings (Cat. No. 00CH37065), Vol. 2, IEEE, 2000, pp. 995–1001.

[164] S. Karaman, E. Frazzoli, Sampling-based algorithms for optimal motion planning, Int. J. Robot. Res. 30 (7) (2011) 846–894.

Nasser Gyagenda received his B.Sc. (Hons.) in Mechanical Engineering at Makerere University, Uganda, in 2010, an M.Sc. in Mechatronics from University of Siegen, Germany, 2015. From 2010–2013, he worked as a design engineer in the Mechanical engineering department of the research and development division of Mühlbauer AG, Roding, Germany. Currently, he is a research assistant and Ph.D. candidate in the department of electrical engineering and computer science at the University of Siegen in Germany. His research interests include mobile robotics and computer vision.

Jasper Hatilima obtained his Bachelor of Engineering degree in Electronics and Telecommunications Engineering at the University of Zambia, Zambia, in 2008. Thereafter, he worked for one of Zambia's mobile network operators from 2008 to 2011 as a Network Performance/Tuning Engineer. He then received his Master of Engineering (MEng) degree in Communication and Information Systems from Southwest Jiaotong University, China, in 2013. He is currently doing his Ph.D. in robotic at the University of Siegen in Germany. His research interests include robot navigation, machine learning, embedded control and low-power edge AI.

Hubert Roth received his diploma and Ph.D. in electrical engineering at the University of Karlsruhe in 1979 and 1983 respectively. From 1983–1988 he worked as a Systems Engineer at Dornier System GmbH, Friedrichshafen, Germany. From 1988–2001 he was Professor at the University of Applied Sciences Ravensburg-Weingarten. Since 2001 Prof. Roth is head of the Institute of Automatic Control Engineering at the University Siegen. He is a Member of the IFAC Technical Committee on Sensor Components and Instruments and Honorary Professor at the Polytechnic in Timisoara, Romania. He was a visiting Professor at the University of London and King's College, London.

Vadim Zhmud graduated from Novosibirsk State Technical University (NSTU) in 1981, defended Candidate and Doctor dissertations in NSTU, worked in the Institute of Automatics and Electrometry SB RAS, in Institute of Laser Physics SB RAS, in Novosibirsk Institute Program Systems (to present day, but part-time) and in NSTU. Presently, he is a full professor with the Department of Automatics, Faculty of Automatics and Computer Techniques, NSTU. His research interests include adaptive and optimal control, multi-channel control systems, laser physics, robotics, and electronics.